Date: October 12, 2011

The right-handed sneutrino as thermal dark matter in U(1) extensions of the MSSM

G. Bélanger[1], J. Da Silva[1] and A. Pukhov[2]

1) LAPTH, Univ. de Savoie, CNRS, B.P.110, F-74941 Annecy-le-Vieux Cedex, France
2) Skobeltsyn Inst. of Nuclear Physics, Moscow State Univ., Moscow 119992, Russia

Abstract

We investigate the parameter space of a supersymmetric model with an extended U(1) gauge symmetry in which the RH sneutrino is a thermal dark matter candidate. In this scenario, annihilation of RH sneutrinos proceeds mainly through Higgs or Z' exchange. We find that sneutrinos in the mass range from 50GeV to more than 1 TeV can be consistent with both the WMAP limit and the direct detection upper limits. Powerful constraints from new gauge boson searches at the LHC as well as from ΔM_s are incorporated. Depending on the choice of the U(1) charge, these scenarios will be further probe by direct dark matter searches as well as by Higgs searches at the LHC.

arXiv:1110.2414v1 [hep-ph] 11 Oct 2011

1 Introduction

The minimal supersymmetric standard model (MSSM) contains two neutral weakly interacting particles that could be dark matter (DM) candidates, the neutralino and the sneutrino. While the neutralino has been extensively studied and remains one of the favorite DM candidates [1–5], the left-handed sneutrino faces severe problems. The sneutrino coupling to the Z boson induces a cross section for elastic scattering off nuclei that can exceed the experimental limit by several orders of magnitude [6]. In particular latest bounds from CDMS [7] or Xenon [8] cannot be satisfied even for a LH sneutrino mass above 1TeV. Furthermore the sneutrino annihilation rate is usually too rapid to provide enough dark matter [6].

The observation of neutrino oscillations indicative of massive neutrinos gives a natural motivation for adding a right-handed (RH) neutrino to the SM fields. Extending the MSSM with RH neutrinos and their supersymmetric partners provides then an alternate DM candidate, the right-handed sneutrino (RHSN). The smallness of the neutrino masses is usually explained by introducing Majorana mass terms and making use of the see-saw mechanism. The natural scale for the RH neutrinos is generally around 10^{12} GeV so that RH neutrinos are too heavy to play a direct role in physics below the TeV scale and so are their supersymmetric partners. Note however that the inverse see-saw mechanism proposes scenarios with RH Majorana neutrinos at the TeV scale [9, 10]. We will not consider these scenarios. It is also possible to generate neutrino masses through Dirac mass terms at the expense of introducing some large hierarchy among the fermions. In this case the supersymmetric partners of the neutrinos are expected to be, as for other sfermions, at the SUSY breaking scale, i.e. around or below 1TeV. In this framework the RH sneutrino can be the lightest supersymmetric particle (LSP). This is the scenario we will consider here.

To make a RHSN LSP a viable dark matter candidate requires special conditions. The RH sneutrino being sterile under standard model gauge interactions cannot be brought into thermal equilibrium.[1] Nevertheless several proposals for sneutrino dark matter have emerged including mixed sneutrinos [15–19], RHSN in models with Dirac mass terms that result from the decay of thermal equilibrium MSSM particles [11, 12], DM from a RH sneutrino condensate [20], sneutrinos in inverse see-saw models [21–24] or RHSN in extensions of the MSSM [25–30]. Extending the gauge group provides another alternative as the RHSN can reach thermal equilibrium because it couples to new vector and/or scalar fields [24, 31, 32]. For example an additional U(1)' gauge symmetry provides new couplings of the sneutrino with the Z' as well as to new scalar fields. In this framework annihilation of pairs of RH sneutrino can be efficient enough to obtain $\Omega h^2 \approx 0.1$. The annihilation is specially enhanced when the particle exchanged in the s-channel is near resonance. Furthermore the elastic scattering cross section of the RHSN is naturally suppressed by several orders of magnitude as compared to the MSSM sneutrino as on the one hand the couplings to the EW scale particles (the Z and the light Higgs) are strongly suppressed and on the other hand the Z' exchange is suppressed because its mass is above the TeV scale. This is the framework that we will study here.

Models with extended gauge symmetries are well motivated within the context of superstring models [33], grand unified theories [34, 35] or little Higgs models [36, 37]. Furthermore in its supersymmetric version, the additional U(1)' symmetry provides an elegant solution to the μ problem. Indeed as in the NMSSM [38] the effective μ parameter is related to the vev of the singlet S responsible for the breaking of the U(1)' symmetry [39, 40]. Another interesting feature of supersymmetric models with extended U(1) symmetry is that a $\lambda S H_u H_d$ interaction allows for the strong first order phase transition that is needed for electroweak baryogenesis [41]. Finally the light Higgs mass is generally above that of the MSSM light Higgs and thus above the direct limit from LEP [42]. Indeed in addition to MSSM-like contributions from squarks and quarks, the light Higgs mass receives contributions from the superpotential (as in the NMSSM) [43] as well as from U(1)' D terms.

In the MSSM with U(1) extended gauge symmetries (UMSSM), the dark matter candidate can either be the neutralino or the sneutrino. The neutralino was investigated in [44–46]. We rather concentrate on the RHSN LSP. The RHSN dark matter was considered in singlet extensions of the MSSM [27, 47] in hybrid inflationnary models [48] as well as in different set-ups [26, 49] or in models with inverse seesaw [22]. Sneutrino dark matter in different U(1) extensions of the MSSM was also examined in [31] and in [50]. Their signatures in cosmic rays [28, 50] or neutrino telescopes [51] were also explored.

In [31] sneutrinos annihilation trough Z' exchange and $\tilde{B}'$ t-channnel exchange into neutrinos were considered while the interactions through the Higgs sector were included in [28, 50]. We extend those analyses by including all possible annihilation and co-annihilation channels and by performing a complete exploration of the parameter space allowing for different choices of the U'(1) symmetry within the context of an E_6 unified model. Furthermore we take into account recent LHC results on the Z', on supersymmetric particles and on the Higgs sector. Insisting on having a sneutrino LSP, to complement previous studies that had concentrated on the neutralino case, will lead to some constraint on the parameter space. In particular the parameters μ and M_1, M_2 have to be larger

[1] Note however that non thermal mechanisms can make a mostly sterile sneutrino a good dark matter candidate [11–14].

than the sneutrino mass in order to avoid a higgsino or a gaugino LSP. We will generically consider only cases with colored sparticles above the TeV scale to easily avoid LHC limits on squarks.

Within the UMSSM with a RHSN dark matter candidate, we found a variety of annihilation channels for the sneutrino, with a predominance of annihilations near a resonance. The main annihilation processes can be classified as

- Annihilation near a light Higgs resonance
- Annihilation near a heavy Higgs resonance
- Annihilation near a Z_2 resonance
- Annihilation into W/Z pairs through Higgs exchange
- Coannihilation with the NLSP, here the NLSP can be neutralino, chargino, charged slepton or any other sfermion.

Note that annihilation into neutrinos can occur either through Z_2 exchange or through $\tilde{B}', \tilde{S}$ exchange when the latter are near the mass of the LSP. The neutrino channels are however never the dominant ones. Finally annihilation of sneutrinos into pairs of new gauge bosons could also contribute, we will not consider this channel here as it is relevant only for sneutrino heavier than the Z', that is above the TeV scale. For such a heavy sneutrino to be the LSP means that all soft parameters are also above the TeV scale. These configurations for supersymmetric particles have a restricted parameter space. For example, very large values of μ often lead to a light Higgs mass below the current limits. Furthermore when the sneutrino is heavier than the Z', the neutralino can become the LSP. We therefore choose rather to concentrate on the subTeV scale sneutrinos. For each scenario we also include an analysis of the direct detection rate as the spin independent cross section of sneutrinos on nucleons turns out to pose severe constraints on a whole class of U(1)' models.

This paper is organized as follows. In section 2 we describe the various sectors of the model as well as the main particle physics constraints. Section 3 presents the relic abundance and section 4 the direct detection rate. Section 5 contains the results for two sample U(1)' models, the $U(1)_\psi$ and $U(1)_\eta$ models, as well as results from a global analysis of the parameter space. Our conclusions are contained in Section 6, while details on the Higgs mass matrices are presented in the Appendix.

2 The model

The symmetry group of the model is $SU(3)_C \times SU(2)_L \times U(1)_Y \times U(1)'$. For definiteness, we assume that this model is derived from an E_6 model, in this case the most general U(1)' charges of fermions are described by only one parameter, θ_{E_6},

$$Q' = \cos\theta_{E_6} Q_\chi + \sin\theta_{E_6} Q_\psi, \tag{1}$$

where $-\pi/2 \leq \theta_{E_6} \leq \pi/2$ and Q_χ, Q_ψ are the generators of two U(1) subgroups of E_6 [32]. The charges of the MSSM left-handed fermions as well as that of the right-handed neutrino are defined in Table 1.

We also assume that the exotic (s)fermions that belong to the fundamental representation of E_6 and that are needed for anomaly cancellation are above the TeV scale. We will neglect them in the following. The only exception is the RH neutrino/sneutrino. We choose the normalization of the coupling constants such that $g_1' = \sqrt{5/3} g_Y$ where g_Y and g_1' are the coupling constants of $U(1)_Y$ and $U(1)'$ respectively and $g_Y = e/c_W$. For the detailed phenomenological analysis we will consider two values of the θ_{E_6} angle corresponding to $\theta_{E_6} = \pi/2$, Q_ψ and $\theta_{E_6} = -.29\pi$ ($\tan\theta_{E_6} = -\sqrt{5/3}$), Q_η. The first choice corresponds to the U(1) subgroup in the breaking of $E_6 \to SO(10) \times U(1)_\psi$. The second choice is used as an example of a scenario in which the sneutrino dark matter candidate differs significantly from the case of the $U(1)_\psi$ model. Note that the RH sneutrino decouples when $\theta_{E_6} = .42\pi$ and that for $\theta_{E_6} = 0$ the symmetry cannot be broken by the singlet field, S, as is the case for other U(1)' models.

Table 1: Charges of the left-handed fermions under $U'(1)$.

	Q	u^c	d^c	L	e^c	ν^c	H_u	H_d	S
$\sqrt{40}Q_\chi$	-1	-1	3	3	-1	-5	2	-2	0
$\sqrt{24}Q_\psi$	1	1	1	1	1	1	-2	-2	4
$2\sqrt{15}Q_\eta$	-2	-2	1	1	-2	-5	4	1	-5

In addition to the MSSM superfields, the model contains a new vector superfield, B', and a new singlet scalar superfield, S. The superpotential is the same as in the MSSM with $\mu = 0$ but has an additional term involving the singlet,

$$W = W_{MSSM}|_{\mu=0} + \lambda S H_u H_d \tag{2}$$

The vev of S, $\langle S \rangle = v_s/\sqrt{2}$ breaks the U(1)' symmetry and induces a μ term

$$\mu = \lambda v_s/\sqrt{2}. \tag{3}$$

The physical fields of the model are those of the MSSM with in addition a gauge boson, Z', and its associated gaugino, $\tilde{B}'$, a scalar field, S, and a neutral higgsino, $\tilde{S}$. This leads altogether to 6 neutralinos and to a Higgs sector with 3 CP-even scalars, 1 CP-odd pseudoscalar and a charged Higgs. Each sector of the model that will play a role in dark matter annihilation is described below.

2.1 Gauge bosons

The two neutral massive gauge bosons, Z^0 and Z' can mix both through mass and kinetic mixing [32, 44]. In the following we will neglect the kinetic mixing as it is not directly relevant to our analysis. The electroweak and U(1)' symmetries are broken respectively by the vev's of the doublets, $v_u/\sqrt{2} = \langle H_u \rangle, v_d/\sqrt{2} = \langle H_d \rangle$ and singlet. The mass matrix reads

$$M_Z^2 = \begin{pmatrix} M_{Z^0}^2 & \Delta_Z^2 \\ \Delta_Z^2 & M_{Z'}^2 \end{pmatrix}. \tag{4}$$

where

$$\begin{aligned} M_{Z^0}^2 &= \frac{1}{4} g_1^2 (v_u^2 + v_d^2) \\ M_{Z'}^2 &= {g'_1}^2 (Q_1^2 v_d^2 + Q_2^2 v_u^2 + {Q'}_S^2 v_s^2) \end{aligned} \tag{5}$$

and we have defined $Q_1 = Q'_{H_d}$, $Q_2 = Q'_{H_u}$, and $g_1 = e/s_W c_W$. Invariance of the superpotential imposes the condition, $Q'_S = -(Q_1 + Q_2)$. The mixing term

$$\Delta_Z^2 = -\frac{1}{2} g_1 g'_1 (Q_1 v_d^2 - Q_2 v_u^2) \tag{6}$$

Diagonalisation of the mass matrix leads to two eigenstates

$$\begin{aligned} Z_1 &= \cos\alpha_Z Z^0 + \sin\alpha_Z Z' \\ Z_2 &= -\sin\alpha_Z Z^0 + \cos\alpha_Z Z' \end{aligned} \tag{7}$$

where the mixing angle is defined as

$$\sin 2\alpha_Z = \frac{2\Delta_Z^2}{M_{Z_2}^2 - M_{Z_1}^2} \tag{8}$$

and masses of the physical fields

$$M_{Z_1,Z_2}^2 = \frac{1}{2}\left(M_{Z^0}^2 + M_{Z'}^2 \mp \sqrt{\left(M_{Z^0}^2 + M_{Z'}^2\right)^2 + 4\Delta_Z^4} \right) \tag{9}$$

. The mixing angle is constrained from precise measurements of Z^0 properties to be of the order or smaller than 10^{-3} [52], the new gauge boson Z_2 will therefore have approximately the same properties as the Z'. As input parameters we choose the physical masses, $M_{Z_1} = 91.187$GeV, M_{Z_2} and the mixing angle, α_Z. From these together with the coupling constants, we extract both the value of $\tan\beta = v_u/v_d$ and the value of v_s. Note that the W mass is a parameter derived from the Z^0 boson mass, $M_W = M_{Z_0}\cos\theta_W$. When $M_{Z_2} \gg M_{Z_1}$ and $\alpha_Z << 1$, the value of $\tan\beta$ is the solution of the following equation

$$\cos^2\beta(-Q_1 + Q_2\tan^2\beta) \simeq \frac{g_2\cos\theta_W}{4g'_1}\sin\alpha_Z\frac{M_{Z_2}^2}{M_W^2} \tag{10}$$

For each U(1)' model, the value of $\tan\beta$ is strongly constrained from the lower bound on the Z_2 mass and on its mixing. For example for $U(1)_\psi$ with $\sin\alpha_Z > 0$, the value of $\tan\beta$ has to be below 1, this is because $\Delta_Z^2 \sim 1 - \tan^2\beta$. Large values of $\tan\beta$ are found when $\sin\alpha_Z < 0$. The large values of $\tan\beta$ are constrained as they this might require too large a mixing angle for a given Z_2 mass. For $U(1)_\eta$, $\Delta_Z^2 \sim 4\tan^2\beta - 1$, therefore $\tan\beta < 0.5$ when $\sin\alpha_Z < 0$. One might think that small values of $\tan\beta$ are problematic for the Higgs mass, however as we will see below additional corrections to the light Higgs mass can bring it above 114 GeV.

2.2 Higgs sector

The CP even mass matrix is obtained after minimization of the potential. The Higgs sector of the UMSSM is described in [53] . We expand the Higgs field as

$$H_d^0 = \frac{1}{\sqrt{2}}\left(v_d + \phi_d + i\varphi_d\right) \tag{11}$$

$$H_u^0 = \frac{1}{\sqrt{2}}\left(v_u + \phi_u + i\varphi_u\right) \tag{12}$$

$$S = \frac{1}{\sqrt{2}}\left(v_s + \sigma + i\xi\right), \tag{13}$$

The squared mass in the ϕ_d, ϕ_u, σ basis both at tree level and including the dominant radiative corrections from top quarks and stops is listed in Appendix A [53]. This squared mass matrix is diagonalized by the transformation $M_D = Z_h \mathcal{M} Z_h^{-1}$ and the mass eigenstates (ordered in mass) are $(h_1, h_2, h_3)^T = Z_h^T(\phi_d, \phi_u, \sigma)^T$.

There is only one pseudoscalar Higgs which is obtained after diagonalizing the 3×3 pseudoscalar mass matrix listed in Appendix A. This matrix is diagonalized by the unitary transformation $M_D = Z_A \mathcal{M}_A Z_A^{-1}$ with the physical pseudoscalar, $A^0 = Z_{A1}\varphi_d + Z_{A2}\varphi_u + Z_{A3}\xi$. The tree-level mass

$$m_A^2 = \frac{\sqrt{2}\lambda A_\lambda}{\sin 2\phi} v \tag{14}$$

and $\tan\phi = v \sin 2\beta / 2v_s$. When $v_s >> v$, the pseudoscalar mass reduces to

$$m_A^2 \simeq \frac{\mu A_\lambda}{\sin\beta\cos\beta} \tag{15}$$

The full matrix including one-loop corrections is also listed in Appendix A together with the corrections to the charged Higgs mass.

Typically the Higgs spectrum will consist of a standard model like light CP-even Higgs, a heavy mostly doublet scalar which is almost degenerate with the pseudoscalar and the charged Higgs, and a predominantly singlet scalar. Note that the mass of the pure singlet $m_S \approx g_1' Q_s v_s$ and is therefore close to that of M_{Z_2} when $v_s \gg v_u, v_d$, see Eq. 4. The hierarchy in the mass of the heavy doublet and the singlet depends on the parameters of the model. For large values of A_λ and λ (and therefore μ) the mass of the heavy Higgs doublet increases and can exceed that of the singlet. Furthermore the Higgs mixing increases, however the singlet component of the light state is usually not large enough to significantly relax the bound on the lightest Higgs contrary to what occurs in the NMSSM [38, 54–56]. Although the lightest scalar Higgs is usually standard model like, it can be significantly heavier than in the MSSM. Indeed the upper bound [53] on the Higgs receives two types of additional contributions as compared to the MSSM, one proportional to A_λ that is also found in the NMSSM, and one from the additional gauge coupling g_1'. The upper bound on the lightest Higgs mass is thus raised to $\mathcal{O}(170)$ GeV [53]. Such a large Higgs mass is however constrained by the latest LHC results which for standard model couplings exclude $m_h > 144$ GeV at the 90%C.L. [57]. The impact of the LHC results on the parameter space of the model will be discussed in more details in [58].

2.3 Sfermions

The important new feature in the sfermion sector is that the U(1)' symmetry induces some new D-terms contributions to the sfermion mass, Δ_f,

$$\Delta_f = \frac{1}{2} g_1'^2 Q'_f \left(v^2 (Q_1 \cos^2\beta + Q_2 \sin^2\beta) + Q'_S v_s^2 \right) \tag{16}$$

where Q'_f are the U(1)' charges of the left fields listed in Table 1. The sfermion mass matrix reads

$$m^2_{\tilde{f}} = \begin{pmatrix} m^2_{\tilde{L}} + (I_f^3 - Q_f s_W^2) M^2_{Z^0} \cos 2\beta + m_f^2 + \Delta_f & m_f (A_f - \mu \tan\beta^{-2I_f^3}) \\ m_f (A_f - \mu \tan\beta^{-2I_f^3}) & m^2_{\widetilde{f_R}} - Q_f s_W^2 M^2_{Z^0} \cos 2\beta + m_f^2 + \Delta_{f^c} \end{pmatrix} \tag{17}$$

where Q_f and I_3^f are the charge and isospin of the SM fermions. The new D-term contribution can completely dominate the sfermion mass, especially for large values of v_s. Those are found in particular when $\theta_{E_6} \approx 0$. The D-term contribution can induce negative corrections to the mass, so that light sfermions can be found even when the soft masses are set to 2TeV. For $\theta_{E_6} > 0$, $\Delta_\nu < \Delta_{Q,u_R,e_R} < \Delta_{L,d_R}$ so that a universal soft mass term for the sfermions at the weak scale naturally leads to a RH sneutrino as the lightest sfermion. Furthermore the NLSP will be the right-handed slepton or the t-squarks if a large mixing decreases the mass of the lightest $\tilde{t}$. On the other hand for $\theta_{E_6} < 0$, $\Delta_\nu > \Delta_{Q,u_R,e_R} > \Delta_{L,d_R}$ so the sneutrino cannot be the LSP with universal soft sfermion masses at the weak scale. In general one expects non-universality in sfermion masses at the weak scale even if universality is imposed when the model is embedded in a GUT scale model. In particular the right-handed sleptons, whose RGE's are driven only by U(1) couplings have the smallest soft terms at the weak scale. Therefore as long as Δ_ν is not much larger than for other sfermions, it is still natural that the sneutrino be the lightest sfermion. This is the case for models where $\theta_{E_6} \approx -\pi/2$ since all correction terms are then almost equal. For the sake of reducing the number of free parameters we will in this study assume that the soft sfermion masses are universal at the weak scale safe for that of the RH sneutrino. In some cases we will find a sfermion NLSP that contributes to coannihilation processes. In the $U(1)_\eta$ model the NLSP will be mostly the left-handed slepton or down-type squarks while in the $U(1)_\psi$ model it will be rather right-handed slepton or up-type squarks.

2.4 Neutralinos

The mass terms for the gaugino sector reads

$$\mathcal{L} = -\frac{1}{2} M_1 \tilde{W}\tilde{W} - \frac{1}{2} M_1 \tilde{B}\tilde{B} - \frac{1}{2} M_1' \tilde{B}'\tilde{B}' - M_K \tilde{B}\tilde{B}' + h.c. \tag{18}$$

The neutralino mass matrix in the basis $(\tilde{B}, \tilde{W}^3, \tilde{H}_d, \tilde{H}_u, \tilde{S}, \tilde{B}')$ thus reads

$$M_{\tilde{\chi}^0} = \begin{pmatrix} M_1 & 0 & -M_{Z^0} c_\beta s_W & M_{Z^0} s_\beta s_W & 0 & M_K \\ 0 & M_2 & M_{Z^0} c_\beta c_W & -M_{Z^0} s_\beta c_W & 0 & 0 \\ -M_{Z^0} c_\beta s_W & M_{Z^0} c_\beta c_W & 0 & -\mu & -\mu v s_\beta / v_s & Q_1 g_1' v c_\beta \\ M_{Z^0} s_\beta s_W & -M_{Z^0} s_\beta c_W & -\mu & 0 & -\mu v c_\beta / v_s & Q_2 g_1' v s_\beta \\ 0 & 0 & -\mu v s_\beta / v_s & -\mu v c_\beta / v_s & 0 & Q_S' g_1' v_s \\ M_K & 0 & Q_1 g_1' v c_\beta & Q_2 g_1' v s_\beta & Q_S' g_1' v_s & M_1' \end{pmatrix}. \tag{19}$$

The mixing matrix is defined such that the lightest neutralino is written as

$$\tilde{\chi}_1^0 = N_{11}\tilde{B} + N_{12}\tilde{W}^3 + N_{13}\tilde{H}_d + N_{14}\tilde{H}_u + N_{15}\tilde{S} + N_{16}\tilde{B}' \tag{20}$$

Note that $v_s >> v$ so that one expects a large mixing between the singlino and $\tilde{B}'$. The chargino sector is identical to that of the MSSM.

2.5 Constraints on the model

The main constraints on the model arise from the gauge boson and Higgs sector. Since colored supersymmetric particles do not play a direct role in sneutrino annihilation, we will generally assume that they are above the TeV scale thus evading the LHC constraints [59, 60].

The Z_2 can be produced directly in pp and $p\bar{p}$ collisions and is searched primarily using leptonic decay modes. The limits from the LHC released earlier this year have superseded the Tevatron limits [52]. We will use the ATLAS exclusion limits published in [61] obtained with an integrated luminosity of $\mathcal{L} = 1.01(1.21) fb^{-1}$ in the $e^+e^-(\mu^+\mu^-)$ channels. These limits are extracted using different U(1)' models, in the two models we will consider for the phenomenological analysis the bounds are similar, with $M_{Z_2} > 1.49$TeV for $U(1)_\psi$ and $M_{Z_2} > 1.54$ TeV for $U(1)_\eta$. These bounds were derived assuming the Z_2 decays only into SM particles. In our case, the Z_2 can also decay into supersymmetric particles, into RH neutrinos and into Higgses, thus reducing the branching ratio into e, μ. For example in the $U(1)_\psi$ model the decays into supersymmetric particles can reach up to 20% especially in cases where the sneutrino is light (hence neutralinos can be light as well) while decays into neutrinos are typically below 10%. In the $U(1)_\eta$, the decays into SM particles is even more suppressed, it never exceeds 65%. This is mainly due to a large branching fraction into right-handed neutrinos (around 30%) as well as into other sparticles. The limits on the Z_2 mass are therefore weakened. To take this effect into account we have computed the modified leptonic branching ratio for each point in our scans and have re-derived the corresponding ATLAS limit.

Another important constraint on the gauge boson sector comes from precision measurements at the Z-pole and from low energy neutral currents. These provide stringent constraints on the mixing angle α_Z. Depending on the model parameters the constraint are below a few 10^{-3} [52]. We will typically set the mixing angle to $|\alpha_Z| = 0.001$.

The Higgs sector is also severely constrained, a standard model like Higgs is constrained by LEP to be above 114 GeV [62] and by LHC searches to be below 144GeV [57]. These

limits can be relaxed when the Higgs couplings to gauge bosons is reduced due to the mixing with the singlet. In the parameter space explored, the singlet component is small and the limit is not modified significantly. The upper limit can also be relaxed if the Higgs has a large branching fractions into invisible particles. The relic density constraint imposes that light sneutrinos have a mass very near $M_{h_1}/2$. Despite a phase space suppression factor, the contribution of the invisible mode to the light Higgs decay can in some cases reach 90% for light sneutrinos, thus relaxing the constraint on the lightest Higgs. When imposing a limit on the light Higgs mass, we have folded in the effect of the invisible decay modes therefore allowing in a few cases a light Higgs heavier than 144 GeV.

Observables in the B sector provide powerful constraints on the supersymmetric parameter space assuming minimal flavour violation. The mass differences of B mesons, $\Delta M_s, \Delta M_d$ have been measured to be $17.77 \pm .12 ps^{-1}$ and $0.507 \pm .004 ps^{-1}$ [62] , somewhat below the SM predictions

$$\begin{aligned} \Delta M_s^{SM} &= 20.5 \pm 3.1 ps^{-1} \\ \Delta M_d^{SM} &= 0.59 \pm 0.19 ps^{-1} \end{aligned} \tag{21}$$

Additional supersymmetric contributions of the same sign as the SM ones are therefore strongly constrained, even though there are large uncertainties in the SM prediction mainly due to the CKM matrix elements and hadronic parameters. Supersymmetric contributions include box diagrams with charged Higgs and quarks, squark/chargino, neutralino and or gluino loops [63] as well as double penguin diagrams with a neutral Higgs exchange. The latter give a significant contribution for large values of $\tan\beta$ and were not included in our analysis. The former are important at small values of $\tan\beta$ which are often found in the U(1)' model. In particular the charged Higgs/quark box diagram contribution adds to the SM contribution inducing too large values for ΔM_s. The dominant contribution, for small values of $\tan\beta$ is proportional to $x \log x (\cot^4\beta)$, where $x = m_t^2/m_{H^+}^2$. This observable thus constrains severely scenarios with $\tan\beta < 1$. The computation of the mass difference is adapted from the routine provided in NMSSMTools [64]. We have also used the same estimate for the theoretical uncertainties.

Other observables such as $b \to s\gamma, B_S \to \mu^+\mu^-$ or $B \to \tau\nu$ are known to receive large supersymmetric contributions when $\tan\beta$ is large, the heavy Higgs doublet is light and/or the squarks are light. The scenario we will study have heavy squarks, Higgs doublets above several hundred GeV's and feature small to moderate values of $\tan\beta$, we therefore have not included these constraints.

3 Relic abundance of sneutrinos

The RH sneutrino couples very weakly to the MSSM particles, its annihilation is therefore primarily through the particles of the extended sector, the new vector boson, Z_2 and new scalars. The coupling of the RHSN to Z_2 is directly proportional to its U(1)' charge, Q'_ν

$$g_{Z_2\tilde{\nu}_R\tilde{\nu}_R^*} = g'_1 Q'_\nu \cos\alpha_Z \tag{22}$$

This coupling does not depend much on the other parameters of the model since $\cos\alpha_Z \approx 1$. Annihilation of sneutrinos becomes efficient when $m_{\tilde{\nu}_R} \approx M_{Z_2}/2$ since the s-channel processes can benefit from resonance enhancement.

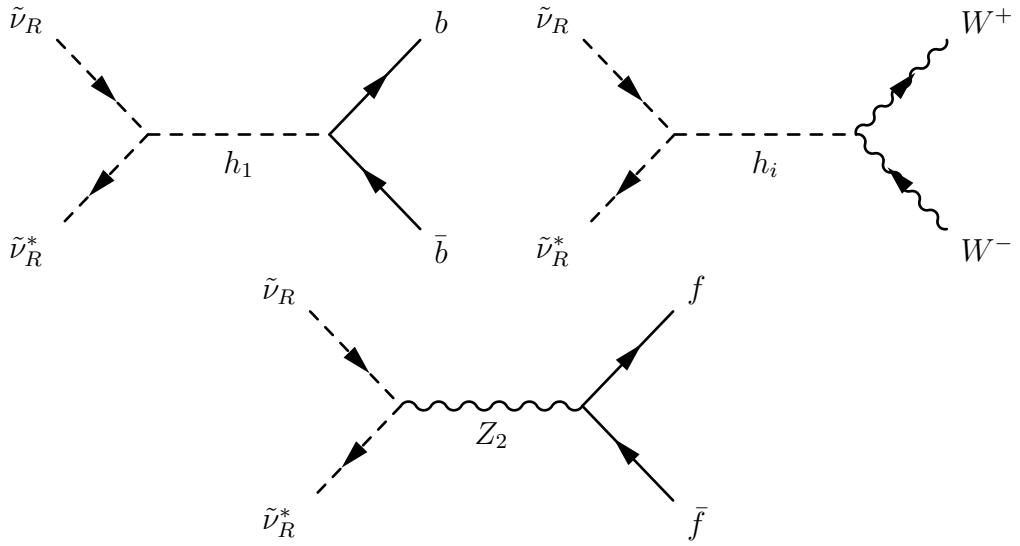

Figure 1: Main annihilation processes for RH sneutrinos.

Sneutrino annihilation also become efficient when $m_{\tilde{\nu}_R} \approx M_{h_i}/2$ where h_i can be any neutral CP even Higgs field. The couplings of the sneutrino to neutral scalars reads

$$g_{h_i\tilde{\nu}_R\tilde{\nu}_R} = -g_1'^2 Q'_\nu \left[v\cos\beta Z_{hi1}Q_1 + v\sin\beta Z_{hi2}Q_2 + v_s Z_{hi3}Q'_s\right]. \tag{23}$$

Since $v_s \gg v$, the largest coupling will be to the predominantly singlet Higgs, for which $Z_{h3i} \approx 1$.Typically the singlet Higgs is the one that has a mass close to Z_2, resonant Higgs annihilation will therefore occur for roughly the same sneutrino mass as the resonant annihilation through Z_2. The light Higgs is dominantly doublet, nevertheless its coupling to sneutrinos receives contributions from all three terms in Eq. 23 since $v_s \gg v$. This coupling is generally sufficient to have a large cross section enhancement near $m_{\tilde{\nu}_R} \approx M_{h_1}/2$. In some cases efficient annihilation can occur away from the resonance, for example annihilation into W/Z pairs through light Higgs exchange or - for heavier RHSN's - into light Higgs pairs or $t\bar{t}$ pairs through singlet exchange. Note that the sneutrino coupling to the lightest Higgs depends on λ (μ), an important parameter to determine the mixing of Higgses. For some choice of parameters, the couplings of the mostly doublet h_1 to the RHSN can be strongly suppressed, not allowing a large enough enhancement on the annihilation cross section. Specific examples will be presented in section 5.

Sneutrinos can also annihilate in neutrino pairs through t-channel exchange of $\tilde{B}'$ in addition to the usual Z_2 contributions. This process contributes mostly for light $\tilde{B}'$ and is never the dominant channel. Finally it is also possible to reduce the abundance of sneutrinos through coannihilation processes, this occur when the masses of the NLSP and the LSP are within a few GeV's. Coannihilation can occur with neutralinos, charginos or other sfermions. Typically, because there is only weak couplings of the RH sneutrino to the rest of the MSSM particles, coannihilation processes involve self-annihilation of the NLSP's and/or NLSP/NNLSP annihilation. The neutralino NLSP will decay via $\tilde{\chi}_1 \to \tilde{\nu}_R\nu_R$ with a typical lifetime of $10^{-19} - 10^{-17}s$ except when it is almost degenerate with the sneutrino LSP which can lead to an increase of lifetime. The NLSP decay will always occur much before BBN and will not spoil its predictions.

To compute the relic abundance we use `micrOMEGAs`2.4 [65]. For this we first imple-

ment the model in LanHEP [66] in both unitary and Feynman gauges and checked gauge invariance for a large number of processes at tree-level. We then introduced radiative corrections to the Higgs masses in the unitary gauge. This code then produces the model file for `CalcHEP` [67] and `micrOMEGAs` [68]. All facilities of `micrOMEGAs` for computing dark matter properties are then obtained automatically, in particular the relic density and the LSP-nucleon scattering cross section. When describing the numerical results we will always impose the condition that the sneutrino is the LSP. For another study of the neutralino LSP as a DM candidate see [44].

4 Direct detection

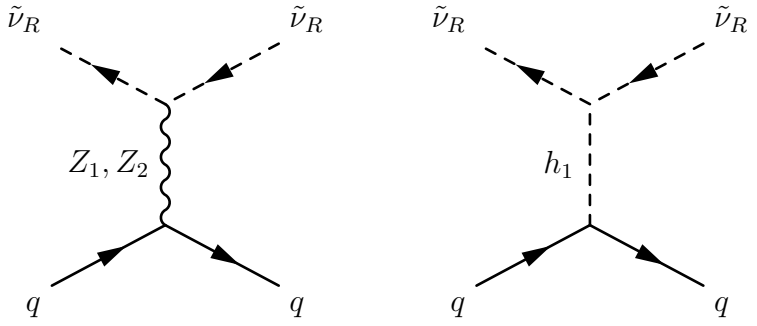

Figure 2: Main scattering processes of the RH sneutrino.

The cross section for scattering of sneutrinos on nucleons will be purely spin independent as the sneutrino is a scalar particle. This process receives contributions from only two types of diagrams: exchange of gauge or Higgs bosons. The gauge boson contribution depends on the vectorial coupling of the fermions to $Z_{1,2}$, with $Q_V^f = I_3 - 2Q\sin^2\theta_W$ for Z^0 and $Q_V'^f = Q'_f - Q'_{f^c}$ for Z'. The total gauge boson contribution to the spin independent cross section on point-like nuclei reads

$$\sigma^{\mathrm{SI,Z}}_{\tilde{\nu}_R N} = \frac{\mu^2_{\tilde{\nu}N}}{\pi}(g'_1 Q'_\nu)^2 \left[\left(y(1-4\sin^2\theta_W)+y'\right)Z + (-y+2y')(A-Z)\right]^2 \tag{24}$$

where

$$\begin{aligned} y &= \frac{g_1}{4}\sin\alpha_Z\cos\alpha_Z\left(\frac{1}{M^2_{Z_2}} - \frac{1}{M^2_{Z_1}}\right) \\ y' &= -\frac{g'_1}{2}Q'^d_V\left(\frac{\sin^2\alpha_Z}{M^2_{Z_1}} + \frac{\cos^2\alpha_Z}{M^2_{Z_2}}\right) \end{aligned} \tag{25}$$

and $Q'^d_V = -4/\sqrt{40}\cos\theta_{E_6}$. The contribution in $1/M^2_{Z_2}$ in y and the one proportional to $\sin^2\alpha_Z$ in y' are always suppressed. From Table 1 one sees that all fermions have a purely axial-vector couplings to Z_ψ and that u-quarks also have purely axial vector couplings to Z_χ. Therefore the Z' contribution is solely dependent on its coupling to d-quarks, hence the term in Q'^d_V in y'. This contribution is expected to be twice as large for neutrons than for protons, see Eq. 24. In the model $U(1)_\psi$, $y' = 0$ and the cross section will depend on the Z_1 exchange contribution. In this case the amplitude for protons is suppressed by a

factor $1 - 4\sin^2\theta_W$ as compared to that for neutrons. Furthermore the Z_1 contribution proceeds through the Z' component so that the cross section is proportional to $\sin^2\alpha_Z$. When $\cos\theta_{E_6} \neq 0$ the term in y' usually dominates by about one order of magnitude for a TeV scale Z_2 and the mixing angle $\alpha_Z = 10^{-3}$. In these scenarios only a weak dependence on α_Z is expected, the largest cross sections are expected for $\theta_{E_6} \simeq 0$ corresponding to the maximal value of $Q_V'^d$.

The Higgs contribution leads to a cross section

$$\sigma^{\mathrm{SI},h}_{\tilde{\nu}_R N} = \frac{\mu^2_{\tilde{\nu}N}}{4\pi} \sum_i \frac{g^2_{h_i\tilde{\nu}_R\tilde{\nu}_R}}{m^4_{h_i} m^2_{\tilde{\nu}_R}} \left((A-Z) \sum_q g_{h_i qq} f^n_q m_n + Z \sum_q g_{h_i qq} f^p_q m_p \right)^2 , \qquad (26)$$

where $g_{h_i qq} = -eZ_{hi1}M_q/(2M_W s_W c_\beta)$ is the Higgs coupling to quarks after the quark mass has been factored out and $g_{h_i\tilde{\nu}_R\tilde{\nu}_R}$ is defined in Eq. 23.

Because of the dependence on the Higgs mass and the fact that the Higgs couplings to quarks goes only through the doublet component, the lightest Higgs doublet generally gives the dominant contribution. Note that the Higgs contribution is inversely proportional to the square of the sneutrino mass and is therefore expected to dominate at low masses since the Z contribution depends only weakly on the sneutrino mass through the effective mass, $\mu_{\tilde{\nu}N}$. Furthermore the Higgs contribution is roughly the same for neutrons and protons. The quark coefficients of the nucleon were taken to be the default values in micrOMEGAS2.4 (with $f^p_{u,d,s} = 0.033, 0.023, 0.26$ and $f^n_{u,d,s} = 0.042, 0018, 0.26$) [69]. There can be large uncertainties in these coefficients, in particular recent lattice results point towards a smaller s-quark coefficient [70], however the quark coefficients will have a significant impact only when the Higgs contribution is dominant, that is for sneutrinos below ≈ 100 GeV.

The total spin independent cross section on point-like nucleus is obtained after averaging over the sneutrino and anti-sneutrino. Note that the interference between the Z and H exchange diagrams have opposite signs for $\tilde{\nu}N$ and $\tilde{\nu}^*N$. Here we assume equal numbers of sneutrino and anti-sneutrinos so that the total cross section is the sum of the Z and H contributions. To compute the direct detection cross section we use `micrOMEGAs`2.4 and thus include all the contributions. To take into account the fact that the proton and neutron contribution are not necessarily equal, we compute the normalized cross-section on a point-like nucleus,

$$\sigma^{\mathrm{SI}}_{\tilde{\nu}_R N} = \frac{4\mu^2_\chi}{\pi} \frac{\left(Z f_p + (A-Z) f_n\right)^2}{A^2} \qquad (27)$$

where the average over $\tilde{\nu}_R$ and $\tilde{\nu}^*_R$ is assumed implicitly. This cross-section can be directly compared with the limits on $\sigma^{\mathrm{SI}}_{\tilde{\chi}p}$ that is extracted from each experiment.

5 Results

The free parameters of the model are $m_{\tilde{\nu}_R}, \mu, M_1, M_2, M_1', M_K, A_\lambda, M_{Z_2}, \theta_{E_6}, \alpha_Z$, as well as all masses and trilinear couplings of sleptons and squarks. To reduce the number of free parameters we fix those that do not belong to the sneutrino or neutralino/Higgs sectors. We thus fix the soft masses of sleptons and squarks to 2 TeV and we take $A_f = 0$ and $A_t = 1$TeV. We furthermore assume $M_1 = M_2/2 = M_3/6$ as dictated by universality at the GUT scale and $M_K = 1$ eV since this parameter mainly affects the $\tilde{B} - \tilde{B}'$ mixing and is

not directly relevant for our study. The remaining free parameters are $m_{\tilde{\nu}_R}, \mu, M_1, M_1', A_\lambda$ and M_{Z_2}, α_Z. We first consider specific choices of θ_{E_6} before letting it be a free parameter.

5.1 The case of the $U(1)_\psi$ model

As we have discussed above, we expect the relic abundance of the sneutrino dark matter to be generally too high. The only ways to bring the abundance within the range preferred by WMAP will be to enhance the annihilation through a resonance effect or make use of coannihilation. We will first describe the typical behaviour of Ωh^2 as a function of the $\tilde{\nu}_R$ mass for fixed values of the free parameters. Once θ_{E_6} is fixed the parameters that have a strong influence on dark matter are M_{Z_2}, the mass of the new gauge boson, A_λ that influence the Higgs spectrum, as well as μ, M_1 that determine the region where the sneutrino is LSP through their influence on the neutralino mass. The parameter μ also influences the Higgs mixing matrix and therefore the coupling of the Higgses to sneutrinos. To limit the number of free parameters we will first fix $M_1 = M_1' = 1$ TeV and rather modify the property of the neutralino NLSP by varying μ. Furthermore allowing to have $\mu < M_1$ will cover the case of the higgsino NLSP which has much higher annihilation cross section than the bino and is therefore more likely to play an important role in coannihilation channels.

5.1.1 A case study with $M_{Z_2} = 1.6$ TeV

We first consider the case where the new gauge boson is just above the LHC exclusion limit, that is $M_{Z_2} = 1.6$ TeV and we fix $\mu = 1$ TeV, $\alpha_Z = -0.001$ and $A_\lambda = 1.5$ TeV. For this choice of parameters, the mass spectrum is such that h_2 is dominantly singlet and has roughly the same mass as the Z_2 while the other heavy Higgses (h_3, A^0, h^+) are nearly degenerate with a mass around 1.97TeV. The light Higgs has a mass of 136.6 GeV and is safely above the LEP limit despite the small value of $\tan\beta = 2.05$. The lightest neutralino has a mass of 957 GeV and is a mixture of bino and higgsino. The sneutrino is therefore the DM candidate when its mass ranges from a few GeV's up to the mass of the lightest neutralino. The value of Ωh^2 lies below the WMAP upper bound in two regions, the first when $60\text{GeV} \leq m_{\tilde{\nu}_R} \leq 69\text{GeV}$ the second when $734\text{GeV} \leq m_{\tilde{\nu}_R} \leq 805\text{GeV}$. In both regions the annihilation cross section is enhanced significantly by a resonance effect. In the first region the h_1 exchange is enhanced and the preferred annihilation channel is into $b\bar{b}$ pairs while in the second region the h_2 and Z_2 exchange are enhanced with a dominant contribution from h_2. The preferred annihilation channels are into $W^+W^-, t\bar{t}, h_1h_1, Z_1Z_1$ pairs, the dominant decay modes of h_2. Note that the decays into gauge bosons proceed through the small doublet component of h_2. For larger masses of the sneutrino, coannihilation with the lightest neutralino can take place. Coannihilation processes involving pairs of neutralinos annihilating through the heavy pseudoscalar Higgs can decrease Ωh^2 such that the WMAP upper bound is satisfied. This occurs when the NLSP-LSP mass difference drops below 60 GeV.

This general behavior is somewhat influenced by our choice of A_λ, μ and α_Z since these parameters influence the masses and mixings of the Higgs doublets and the couplings of sneutrinos to Higgses. For example for $A_\lambda = 100$ GeV, the mass of the heavy doublet (which is now h_2) decreases to 592 GeV. The h_2/A^0 exchange contributes to sneutrino annihilation into top pairs thus leading to a decrease of the value of Ωh^2 as one approaches

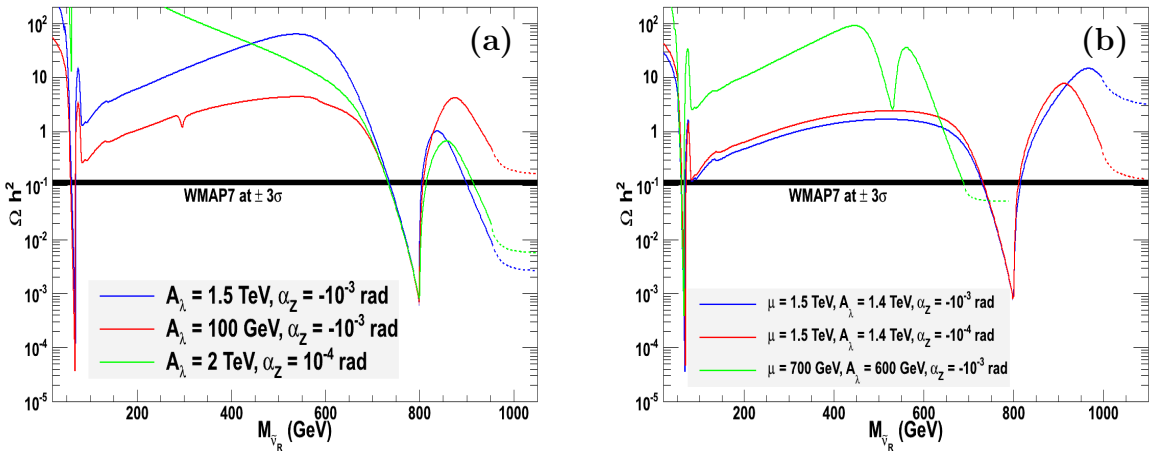

Figure 3: Ωh^2 as a function of the LSP mass for $M_{Z_2} = 1.6$ TeV and (a) $\mu = 1$ TeV, $(A_\lambda(TeV), \alpha_Z) = (1.5, -10^{-3}), (0.1, -10^{-3}), (2., -10^{-4})$ (b) $\mu = 1.5$TeV, $(A_\lambda(TeV), \alpha_Z) = (1.4, -10^{-3}), (1.4, -10^{-4})$ and $\mu = 0.7$TeV, $(A_\lambda(TeV), \alpha_Z) = (0.6, -10^{-3})$. Full (dash) lines correspond to the region where the LSP is the RHSN (neutralino).

the Higgs resonance, the drop is not significant enough to bring the relic density below the WMAP upper bound, see Fig. 3a. As another example consider the case $A_\lambda = 2$ TeV and $\alpha_Z = 10^{-4}$. Here the $h_1\tilde{\nu}_R\tilde{\nu}_R$ coupling is suppressed, Ωh^2 becomes very large and despite a resonance effect when $m_{\tilde{\nu}_R} \approx m_{h_1}/2$ the WMAP upper bound can never be satisfied for a sneutrino lighter than 100GeV, see Fig. 3a.

The parameter μ induces corrections to the light Higgs mass as well as shifts in the Higgs mixing matrix. In particular increasing μ (and therefore λ) to 1.5 TeV increases the singlet mixing in the light Higgs and thus the $\tilde{\nu}_R\tilde{\nu}_R h_1$ coupling. This makes annihilation processes through Higgs exchange more efficient, and gives rise to a new region where Ωh^2 is below the WMAP upper bound when the sneutrino mass is just above the W pair threshold, see Fig. 3b with $A_\lambda = 1.4$ TeV. Note that in this case the lightest neutralino has a large bino component and coannihilation is not very efficient. Lowering μ to 700 GeV, changes the nature of the lightest neutralino which becomes dominantly higgsino with its mass determined by μ. Thus the range of masses where the sneutrino is the LSP becomes narrower. In fact the singlet Higgs/Z_2 pole annihilation region cannot be reached when the sneutrino is the LSP, the region compatible with WMAP is rather one where higgsino coannihilation dominates. In Fig. 3b, one can see a significant drop in Ωh^2 near the h_2 resonance, this is however not sufficient to have efficient annihilation of the RHSN.

The direct detection spin independent (SI) cross section receives contributions from both the light Higgs and Z_1 exchange. In general for the $U(1)_\psi$ scenario, the cross-section is below the limits from Xenon100 [7]. As we have argued above, this is because the Z_1 contribution is directly proportional to $\sin^2\alpha_Z$. This contribution nevertheless dominates for a mixing angle $|\alpha_Z| = 10^{-3}$ except for small masses. It gives $\sigma = 1.4 \times 10^{-10}$ pb for $m_{\tilde{\nu}_R} \geq 200$ GeV and is mostly independent of other input parameters, see Fig. 4a,b. Furthermore the Z_1 contribution is much larger for neutrons than for protons. We take that into account by computing the cross section for scattering on point-

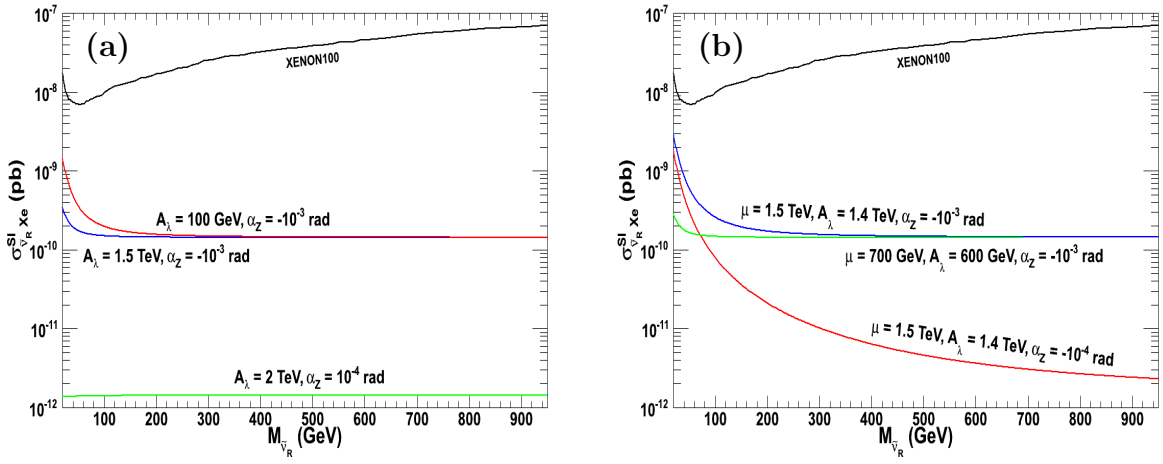

Figure 4: $\sigma^{SI}_{\tilde{\nu}_R N}$ as a function of the LSP mass for the same parameters as Fig. 3. The Xenon100 exclusion curve is also displayed.

like nucleons (here we use Xenon) normalized to one nucleon. For masses in the range $50-100$ GeV, the SI cross section is enhanced due to the light Higgs exchange contribution which increases at low sneutrino masses, although for this scenario the values are always below the experimental limit. The predictions are in the range $\sigma = 2\times10^{-10} - 3\times10^{-10}$ pb for $\alpha = -10^{-3}$. The SI cross section drops rapidly with the mixing angle, for example for $\alpha_Z = |10^{-4}|$, $\sigma^{SI}_{\tilde{\nu}_R N} \simeq 10^{-12}$ pb for $m_{\tilde{\nu}_R} \geq 200$ GeV, see Fig. 4a. For small values of the mixing angle, the Z_1 contribution is suppressed and the Higgs contribution can become dominant even for masses of a few hundred GeV's, this however corresponds to a low overall cross section, see for example Fig. 4b. The spin-independent cross section can be further suppressed in the limit $\alpha_Z = 0$ and for parameters for which the h_1 couplings to sneutrino is suppressed.

5.1.2 Exploration of $U(1)_\psi$ parameter space

After having describe the general behavior of Ωh^2 and of the direct detection rates for some choice of parameters, we now search for the region in parameter space that are compatible with $0.1018 < \Omega h^2 < 0.1228$ corresponding to the WMAP 3σ range [71] as well as with the direct detection limit of Xenon100 [7]. We have further imposed the limits on the Higgs sector from LEP and the LHC and have taken into account the impact of the invisible decay mode of the Higgs. We have also used limits on sparticles from LEP as implemented in `micrOMEGAs` . Note that since we are only considering the case of heavy sfermions, these limits as well as the new LHC limits on sparticle masses do not come into play [59, 60]. Finally we have also imposed the constraints from $\Delta M_{d,s}$. We have performed random scans with 5×10^6 points. The range for the parameters are listed in Table 2. As before we here fix all sfermion masses to 2TeV and neglect all trilinear couplings with the exception of $A_t = 1$ TeV. Note that we impose $\mu > 0$ and therefore consider only positive values for A_λ, see Eq. 15.

The results of the scan as displayed in Fig. 5 show that the allowed values for $m_{\tilde{\nu}_R}$ cover a wide range from 55 GeV to the largest value probed. The allowed points in the plane $m_{\tilde{\nu}_R} - M_{Z_2}$ are clustered in three regions around $m_{\tilde{\nu}_R} \approx 60$ GeV, around

Parameter	Range
$m_{\tilde{\nu}_R}$	[0, 1500] GeV
M_{Z_2}	[1300, 3000] GeV
μ	[100, 2000] GeV
A_λ	[0, 2000] GeV
α_Z	[-0.003, 0.003] rad
M_1, M_1'	[100, 2000] GeV

Table 2: Range of the free parameters in the $U(1)'$ models

$m_{\tilde{\nu}_R} \approx M_{Z_2} - \delta(+\delta')$ with $\delta \approx 70$ GeV($\delta' \approx 10$ GeV), and $m_{\tilde{\nu}_R} \approx 90 - 100$ GeV. The first two are characterized by the main annihilation mechanism near a resonance. The latter corresponds to annihilation through a Higgs exchange. As discussed above, this requires a large value for μ, see Fig. 5b. The remaining allowed scenarios correspond to $m_{\tilde{\nu}_R} \approx m_{\chi_1^0}$. In most cases the NLSP is a higgsino and $m_{\tilde{\nu}_R} \approx \mu$, see Fig. 5b, then important contributions from coannihilation processes involving neutral and charged higgsinos annihilating into fermion pairs are to be added to the sneutrino annihilation processes dominated by the channels into WW, ZZ through Higgs exchange. Because μ is constrained by the LEP limit on charginos, the RHSN mass is in this case heavier than 90 GeV. A few cases where the NLSP has an important bino component are also found, those correspond to the points above the line $\mu \approx m_{\tilde{\nu}_R}$ in Fig. 5b.

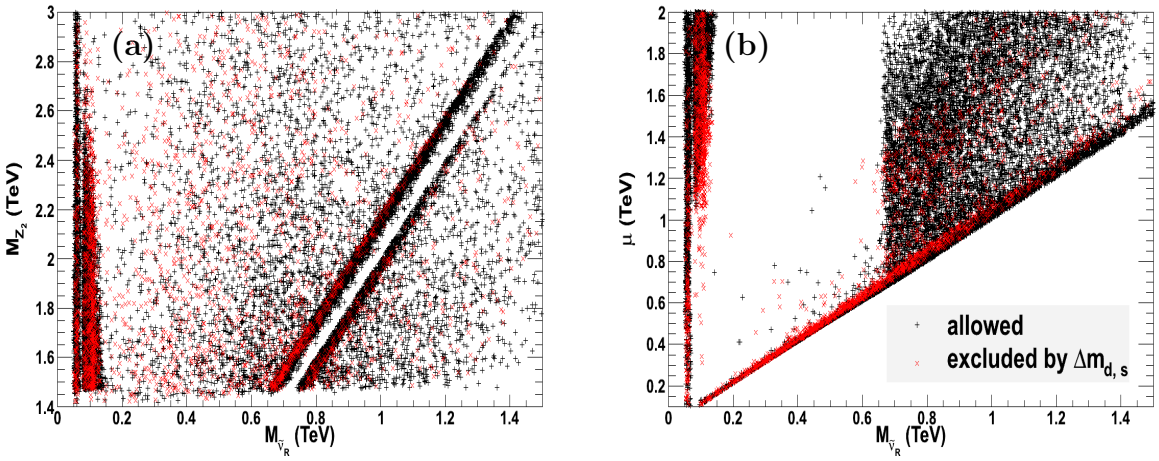

Figure 5: The allowed scenarios in the a) M_{Z_2} vs $m_{\tilde{\nu}_R}$ plane and b) μ vs $m_{\tilde{\nu}_R}$ plane. Points excluded by the $\Delta M_{d,s}$ constraint are displayed in red.

In this model, the cross section for LSP scattering on nuclei is dominated by either Higgs or Z_1 exchange and is mostly independent of M_{Z_2}. The direct detection cross section can reach at most $\sigma^{SI}_{\tilde{\nu}_R N} = 2 \times 10^{-9}$ pb when $m_{\tilde{\nu}_R} \approx 50 - 60$ GeV and the light Higgs exchange dominates while the maximal value is only $\sigma^{SI}_{\tilde{\nu}_R N} \approx 5 \times 10^{-10}$ pb for sneutrinos

above 200 GeV when Z_1 exchange is dominant. These predictions are much below the exclusion limits of XENON100 [7]. Values below $\sigma^{SI}_{\tilde{\nu}_R N} = 10^{-13}$ pb can also be obtained, these occur when the Z_1 contribution is suppressed by the small mixing angle and the light Higgs coupling to the LSP are suppressed as well. Cases where coannihilation processes dominate can also lead to small cross sections.

Constraints from $\Delta M_{d,s}$ rule out some of the parameter space, in particular the case where $\alpha_Z > 0$ since it leads to values of $\tan\beta < 1$. The allowed points in the $\tan\beta - \alpha_Z$ plane are displayed in Fig. 6b. As mentioned in Section 2.5, when $\tan\beta$ is small the charged Higgs box diagram adds to the SM contribution and leads to value for ΔM_s that is too large. This constrain does not influence directly the range of predictions for the direct detection cross section, nor does it affect the range of allowed masses for the RHSN.

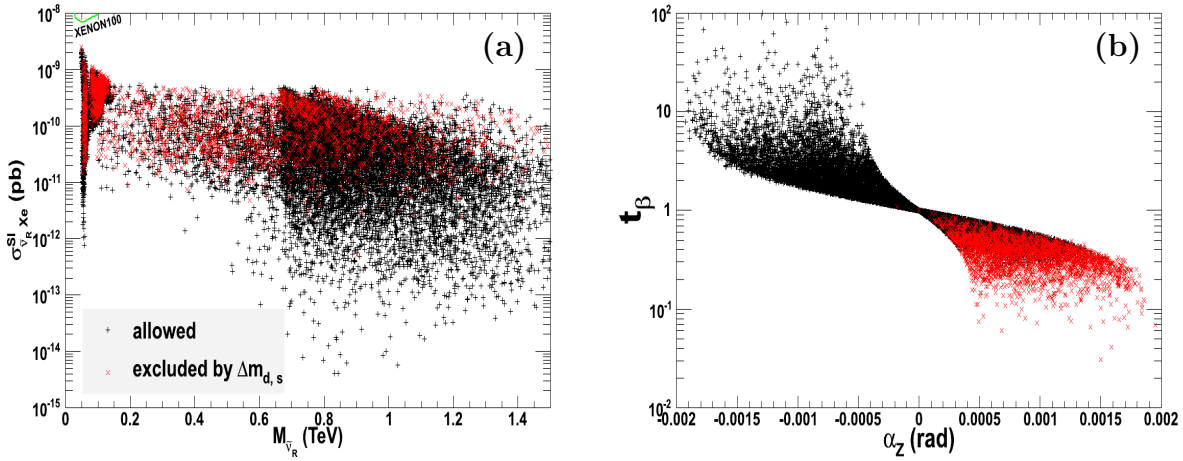

Figure 6: (a) $\sigma^{SI}_{\tilde{\nu}_R Xe}$ as a function of the LSP mass for the allowed scenarios in the $U(1)_\psi$ model. (b) Allowed scenarios in the $\tan\beta$- $m_{\tilde{\nu}_R}$ plane. Points excluded by ΔM_s are displayed in red.

5.2 The case of the $U(1)_\eta$ model

The properties of the RHSN dark matter are dependent on the choice of the U(1)' charges. To illustrate some of the differences we present results for $\theta_{E_6} = -.29\pi$ ($U(1)_\eta$) before discussing arbitrary values in the next section. We chose this model for its phenomenological properties. For this value of θ_{E_6}, the coupling of the sneutrino to Z_2 is enhanced as compared to the previous example with $Q'_\nu = -\sqrt{5}/2\sqrt{3}$. Furthermore the coupling of the RHSN to h_1 is typically enhanced as compared to the model $U(1)_\psi$. Finally the vectorial couplings of Z' to neutrinos and d-quarks are non-zero. Therefore both terms in Eq. 24 can contribute to the SI cross section, this implies a direct detection cross section that is much larger than found previously. Nevertheless the vectorial couplings of Z_1 are far enough from their maximal value that it is possible to find scenarios that satisfy direct detection limits as will be demonstrated below.

5.2.1 A case study with $M_{Z_2} = 1.6$ TeV

To illustrate the behaviour of the relic density and the direct detection rate we choose $M_{Z_2} = 1.6$ TeV, $\alpha_Z = 0.001$, $\mu = 1.5$ TeV and $A_\lambda = 0.5$ TeV. For this choice of parameters $m_{h_1} = 116.9$ GeV despite a small value of $\tan\beta = 1.2$. The doublet Higgses are around 1.3 TeV while h_3 is nearly degenerate with Z_2. As for the the model $U(1)_\psi$, the relic density satisfies the WMAP upper bound in the regions where annihilation into light Higgs or singlet Higgs/Z_2 is enhanced by a resonance effect as well as in a region where annihilation via h_1 exchange is efficient without the benefit of a resonance enhancement. The latter region extends over a wide range of values for the LSP mass because of the large couplings of the sneutrinos to h_1. The preferred annihilation channels are typically into WW, ZZ $t\bar{t}$ or h_1h_1 pairs as well as into $b\bar{b}$ for light sneutrinos. Note also that exchange of h_2 can contribute significantly to sneutrino annihilation, see the small dip at $m_{\tilde{\nu}_R} = 650$ GeV in Fig. 7a. In this scenario the direct detection cross section is large ($\sigma^{SI}_{\tilde{\nu}_R N} \approx 4.5 \times 10^{-8}$ pb for $m_{\tilde{\nu}_R} \geq 100$GeV) and exceeds the Xenon100 bound for a sneutrino LSP below 550 GeV, see Fig. 7b. This is because both the Z_1 and Z_2 contribute significantly to the cross section. Extending the region of validity of sneutrino DM over a larger mass range after considering direct detection limits thus requires decreasing the mixing angle α_Z and/or increasing the mass of the Z_2. For example taking $\alpha_Z = 10^{-4}$, $\mu = A_\lambda = 1.8$TeV has the effect of decreasing the relic density - so that it is below the WMAP upper bound for sneutrino masses in the range 90-900 GeV - while also decreasing the SI cross section. Yet the LSP is still constrained to be $m_{\tilde{\nu}_R} \geq 370$ GeV. In fact the direct detection rate decreases by less than a factor of two, this is because the contribution of the Z_2 exchange, the term proportional to Q'^d_V in Eq. 24, is not suppressed by $\sin\alpha_Z$. This means that to have sneutrino DM with a mass of a few hundred GeV's also requires increasing the mass of the Z_2. For example taking $M_{Z_2} = 2.5$ TeV decreases the direct detection rate below the Xenon100 exclusion for all masses of the LSP. However for this choice of parameters, only light sneutrinos also satisfy the relic density constraint since the heavy sneutrino LSP cannot annihilate through the singlet/Z_2 resonance.

Finally we comment on the coannihilation region. We have fixed $M_1 = 1$ TeV, so that the lightest neutralino has a mass ≈ 1 TeV and is dominantly bino. For values of $\mu \leq 1$ TeV, the lightest neutralino has a large higgsino component and coannihilation is efficient. For the benchmarks with $\mu = 1.5$ TeV the coannihilation processes involving binos are not efficient enough to reduce Ωh^2 to a value compatible with WMAP.

5.2.2 Exploration of $U(1)_\eta$ parameter space

We also explore the parameter space of the model, varying the parameters in the range shown in Table 2. As before, we impose in addition to limits on Ωh^2 and on the SI cross section, the lower limit on the Higgs and Z_2 mass, and the limit on $\Delta M_{d,s}$. The results are displayed in Fig. 8 in the $M_{Z_2} - m_{\tilde{\nu}_R}$ plane, as well as in the $\mu - m_{\tilde{\nu}_R}$ plane. As we have discussed above, because Higgs annihilation is efficient enough, the sneutrinos are not confined to the h_i, Z_2 resonance region. Sneutrinos from 100GeV to $M_{Z_2}/2$ can satisfy the relic density constraint, either through pair annihilation or through coannihilation (the region where $m_{\tilde{\nu}_R} \approx \mu$). In the former case large values of μ are preferred to have large enough couplings of the sneutrino LSP to h_1. The direct detection cross section is large with a maximum value near $\sigma^{SI}_{\tilde{\nu}_R N} \approx 10^{-7}$ pb for the whole range of LSP masses. Because the experimental limits on the direct detection rate are more stringent for masses around

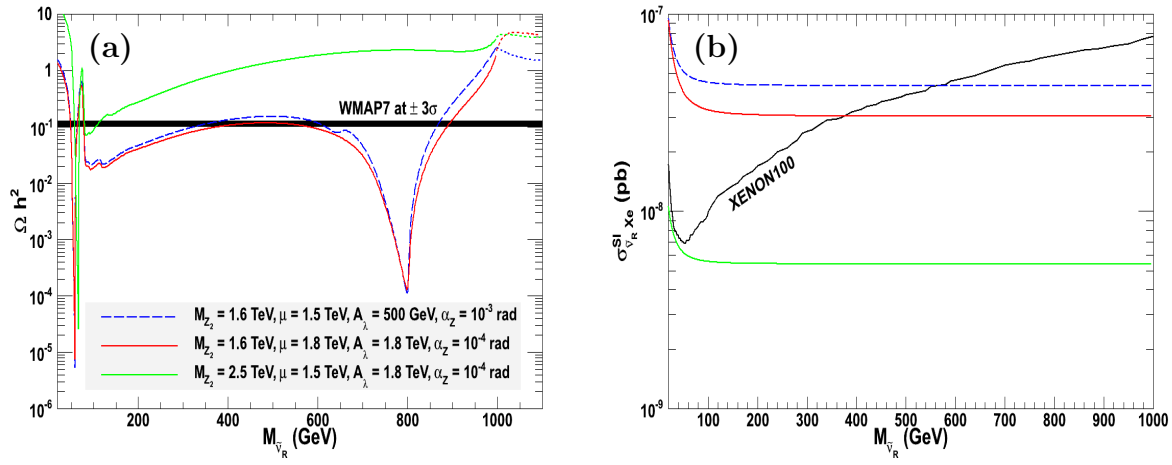

Figure 7: Ωh^2 as a function of the LSP mass for a) $M_{Z_2} = 1.6$ TeV, $\mu = 1.5$ TeV, $A_\lambda = 0.5$ TeV, $\alpha_Z = 10^{-3}$ and $M_{Z_2} = 1.6, 2.5$ TeV, $\mu = 1.8$ TeV, $A_\lambda = 1.8$ TeV, $\alpha_Z = 10^{-4}$. The dotted lines correspond to the neutralino LSP. b) $\sigma^{SI}_{\tilde{\nu}_R N}$ as a function of the LSP mass for the same choice of parameters.

80 GeV, light sneutrinos are severely constrained especially when the Z_2 mass is lighter than 2TeV. The lower bound on the cross section for $M_{Z_2} \leq 3$ TeV is $\sigma^{SI}_{\tilde{\nu}_R N} = 2. \times 10^{-9}$ pb . The typically large direct detection rate is the main signature of this scenario. To completely probe this scenario up to DM masses of 0.3(1.5) TeV requires one (two) orders of magnitude improvement over the current limits. Several of the scenarios are also constrained by ΔM_s, in particular when $\alpha_Z < 0$ which implies $\tan\beta < 1$. This does not affect the range of values of sneutrino masses compatible with all constraints.

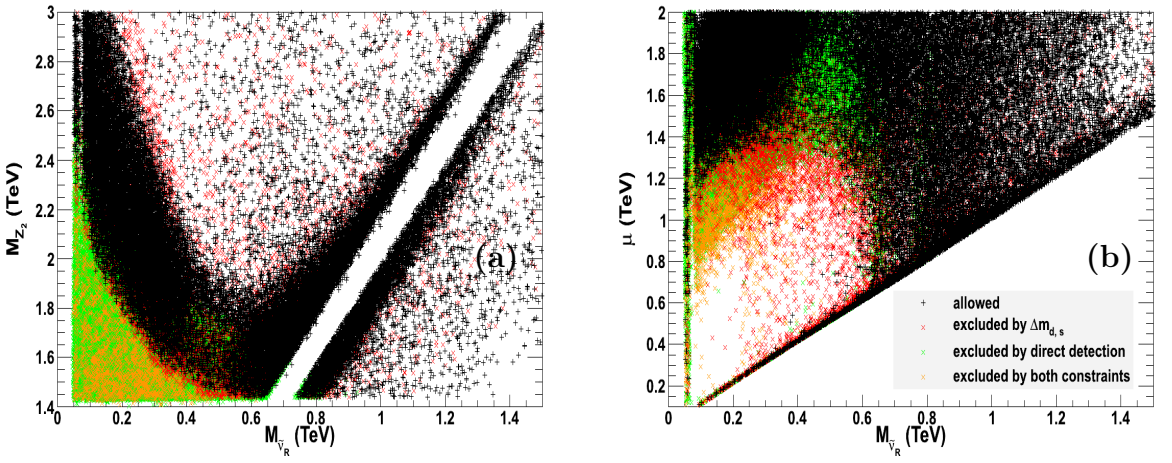

Figure 8: The allowed $U(1)_\eta$ scenarios in the a) M_{Z_2} vs $m_{\tilde{\nu}_R}$ plane and b) μ vs $m_{\tilde{\nu}_R}$ plane. In red, points excluded by the $\Delta M_{d,s}$ constraints, in green those excluded by XENON100 and in yellow those excluded by both constraints.

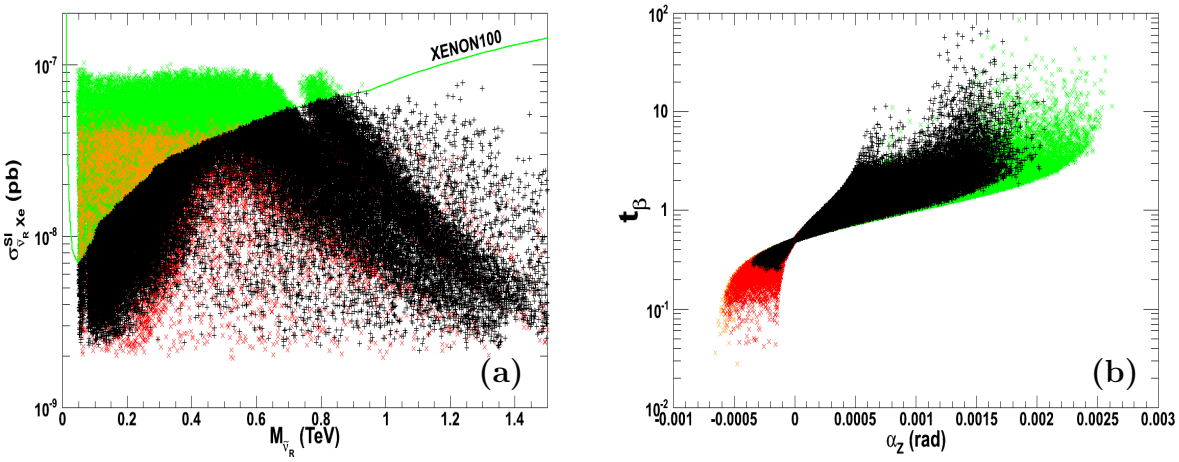

Figure 9: a) $\sigma^{SI}_{\tilde{\nu}_R Xe}$ as a function of the LSP mass for the allowed scenarios in the $U(1)_\eta$ model. b) Allowed scenarios in the $\tan\beta$- α_Z plane, same color code as Fig. 8.

5.3 A global scan of the parameter space

Having illustrated the properties of the sneutrino dark matter in specific models we will next explore the complete parameter space of the model by keeping all parameters for the neutralino, sfermion and gauge boson sector free while imposing the constraints from WMAP, direct detection as well as on Higgs masses.

The values of θ_{E_6} where the sneutrino is a good dark matter candidate are restricted. First for $\theta_{E_6} \approx 0$ the value of v_s becomes very large especially when M_{Z_2} is large. This induces large negative corrections to sfermion masses and lead in particular to a charged LSP. For example, for soft terms at 2TeV the values $-0.2 < \theta_{E_6} < 0.05$ are excluded when $M_{Z_2} = 1.$TeV. Second the direct detection cross section is often too large when $|\theta_{E_6}| < 0.5$. This is due mainly to the contribution of the Z_2 exchange to the direct detection cross section that is proportional to $\cos\theta_{E_6}$. To illustrate this we display the variation of the direct detection cross section as a function of θ_{E_6} for different values of M_{Z_2} in Fig. 10. We choose $m_{\tilde{\nu}_R} = M_{Z_2}/2$ so as to guarantee that the WMAP upper bound is satisfied and fix $\mu = M_{Z_2}/2 + 0.5$ TeV in each case to ensure that the sneutrino is the LSP. We have also fixed $M_{\tilde{f}} = 2$ TeV. The direct detection bound are easily satisfied near $\theta_{E_6} = \pm\pi/2$ because of the suppressed contribution of the Z vectorial coupling, see Fig. 10. The mixing angle α_Z has only a moderate impact on the direct detection rate, while increasing the mass of the M_{Z_2} reduces the SI cross section, except when $\theta_{E_6} = \theta_\psi$ as we have seen in Section 5.1. Note that for $\alpha_z < 0$ there is a dip in the cross section near $\theta_{E_6} = \pi/2$, this is because of a cancellation between the y and y' contributions in Eq. 24 in the cross section on neutrons.

For the random scans we choose the same range as in Table 2 with in addition $-\pi/2 \leq \theta_{E_6} \leq \pi/2$. As before, we have applied the constraints on M_{Z_2} from the LHC and on α_Z. We have imposed the latest constraint from XENON100 [7] and from ΔM_s a posteriori to better illustrate the impact of these constraints. The successful scenarios are displayed in Fig. 11 in the $M_{Z_2} - \theta_{E_6}$ plane. The white region at small values of θ_{E_6} have a charged fermion LSP. Many scenarios with $-\pi/4 < \theta_{E_6} < 0$ have too large a direct detection rate as was the case for the model $U(1)_\eta$. The value of the direct detection cross section

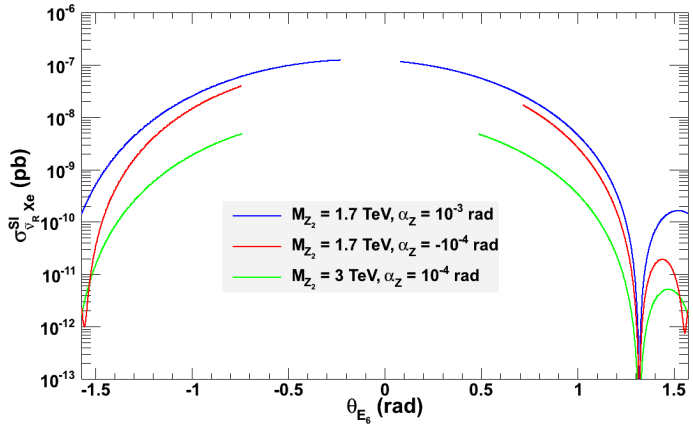

Figure 10: $\sigma^{SI}_{\tilde{\nu}_R N}$ as a function of θ_{E_6} for $(M_{Z_2}, \alpha_Z) = (1.7, 10^{-3}), (1.7, -10^{-4}), (3, 10^{-4})$, $\mu = M_{Z_2}/2 + 0.5$ TeV, $A_\lambda = 1$ TeV and $m_{\tilde{\nu}_R} = M_{Z_2}/2$.

span several orders of magnitude from less than 10^{-13} pb to 2×10^{-7} pb. In particular for sneutrino masses around 100 GeV there are many models which exceed the direct detection limit. These are scenarios with $\theta_{E_6} < 0$ where the sneutrino coupling to light Higgs allows efficient annihilation even away from resonance as discussed in the case of $U(1)_\eta$. The enhanced couplings to the Higgs as well as the coupling to the $Z_{1,2}$ lead to a large direct detection rate. Models with $\theta_{E_6} > 0$ have only light sneutrinos in that mass range when coannihilation plays a role and therefore tend to have much lower direct detection rate. In fact even for heavier masses models with $\theta_{E_6} > 0$ predict smaller direct detection rates as discussed above.

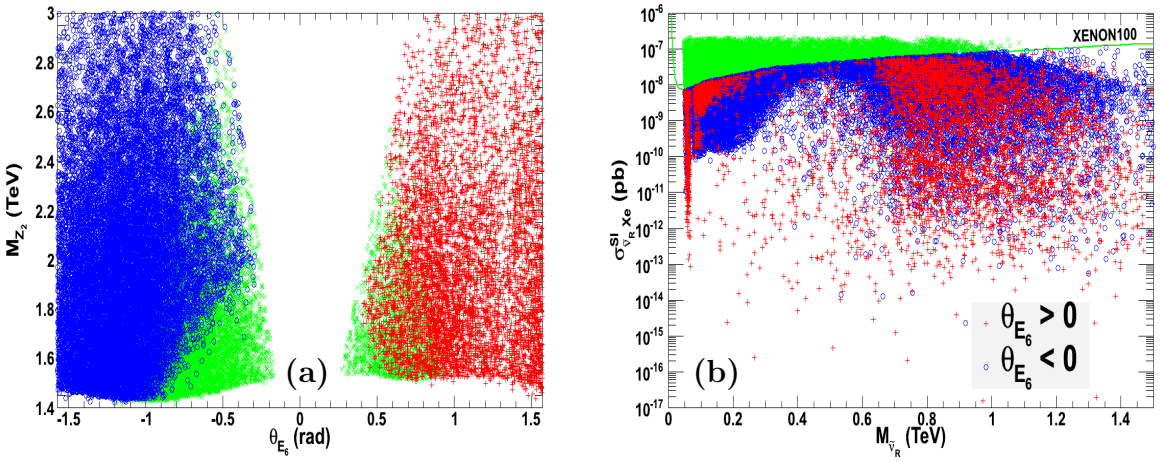

Figure 11: a) Allowed scenarios in the M_{Z_2} vs θ_{E_6} plane, the models above the XENON100 bound are in green (light grey). b) $\sigma^{SI}_{\tilde{\nu}_R N}$ as a function of $m_{\tilde{\nu}_R}$.

The processes that can contribute to Ωh^2 were discussed both in the context of $U(1)_\psi$ and $U(1)_\eta$ models. In the general case we find similar results. We find a predominance of annihilation near a h_1 or singlet Higgs/Z_2 resonance as well as annihilation into gauge boson pairs through h_1 exchange. The latter being confined to sneutrino masses just above the W pair threshold when $\theta_{E_6} > 0$. These regions have a high density of points

in the plane $M_{Z_2} - m_{\tilde{\nu}_R}$ in Fig. 12a. For $\theta_{E_6} > 0$ the only other allowed scenarios have $m_{\tilde{\nu}_R} \approx \mu$ as displayed in Fig. 12b. These are dominated by Higgsino coannihilation. For $\theta_{E_6} < 0$, sneutrinos of masses above 100 GeV can also annihilate efficiently through h_1 exchange provided their coupling to h_1 is large enough - this requires large values of μ. In both figures we have imposed the $\Delta M_{d,s}$ constraint although we do not display explicitly its impact. As discussed in the previous section this constraint plays a role for small values of $\tan\beta$ for any values of the LSP mass.

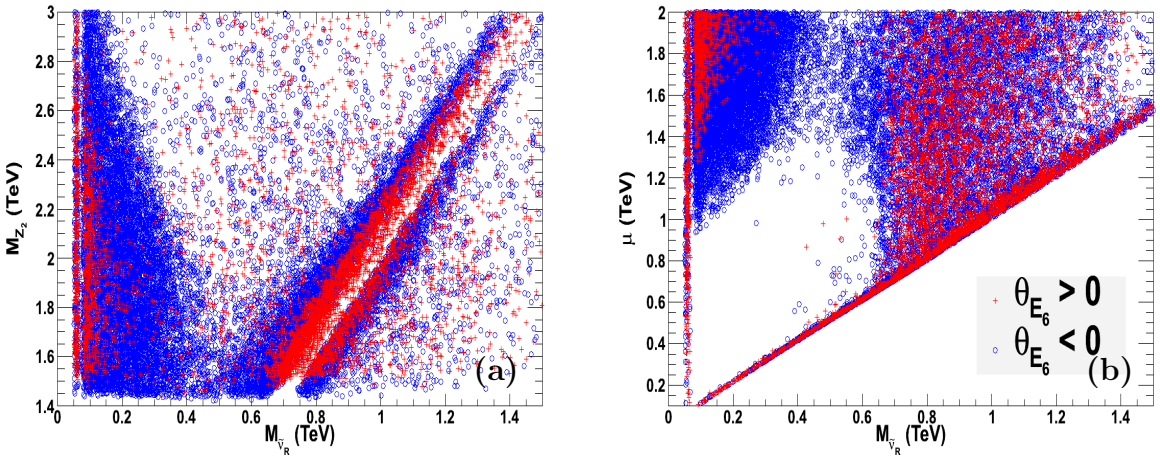

Figure 12: The allowed scenarios in the a) M_{Z_2} vs $m_{\tilde{\nu}_R}$ plane and b) μ vs $m_{\tilde{\nu}_R}$ plane after applying all constraints.

6 Conclusion

The right-handed sneutrino is a viable thermal dark matter candidates in U(1) extensions of the MSSM. The allowed parameter space depends strongly on the value of the new Z_2 vector boson mass. Sneutrino annihilation is typically dominated by resonance annihilation, with in particular the dominant contribution from the Higgs sector rather than from the new gauge boson Z_2. For the light Higgs this requires fine tuning of the masses while for the heavy singlet Higgs the mass difference has to be within 15% (of $m_{h_i}/2$). As in other supersymmetric models, coannihilation processes can also be important. For simplicity we have only discussed the case of one sneutrino dark matter candidate, in the case of complete degeneracy of three sneutrinos the relic density increases by a factor 3. Indeed the annihilation cross section is the same for all sneutrino flavours since there is never a significant contribution from annihilation into neutrino pairs, thus the increase in the number of channels is compensated by the increase in the degrees of freedom leading to a smaller effective annihilation cross section. This will imply a narrower range of masses for the LSP near $M_{h_i}/2$.

The direct detection limit is very stringent for a whole class of models unless the mass of the Z_2 is above 2TeV. These scenarios with $\theta_{E_6} < 0$ will be best tested with SI detectors with improved sensitivities. In particular with a factor of 2 better sensitivity the whole region with intermediate masses for the sneutrinos - when annihilation into W pairs is dominant - will be probed. The scenarios with $\theta_{E_6} > 0$ are more challenging to probe

via direct detection. Another signature of the RHSN model is that of a new gauge boson at the LHC. In fact the recent results from searches for Z_2 gauge bosons at the LHC have had a significant impact on the parameter space of the model and pushed one of the favored region for the sneutrino LSP to be near 800GeV. A Z_2 up to several TeV's will be probed when the energy of the LHC is increased to 14TeV. A negative result from such a search will imply a much reduced rate for direct detection searches as well. Indirect searches could also provide a good probe of the RHSN model, these will be investigated separately.

In this analysis we have assumed that Dirac neutrinos were very light (sub-eV range). Such right-handed Dirac neutrinos can be produced by Z' interactions prior to big bang nucleosynthesis leading to a faster expansion rate of the universe and to too much He^4. The resulting constraints on the mass of the new gauge bosons in the E_6 model were analyzed in [72] and compatibility with BBN resulted into lower limits on the Z' mass in the multi-TeV range assuming the effective number of neutrinos was increased by 0.3. However since then new data from WMAP have been released which implied a higher than expected value for the abundance of He^4 and for the effective number of relativistic neutrino species, more precisely $N_{eff} = 4.34 + 0.86 - 0.88$ [73, 74]. This new value would have the effect of relaxing the lower limit on the Z' mass to a value comparable to LHC bounds.

7 Acknowledgements

G.B. thanks the LPSC, Grenoble for its hospitality. We thank S. Viel for discussions on the LHC bounds on new gauge bosons. This work was supported by the GDRI-ACPP of CNRS. The work of AP was supported by the Russian foundation for Basic Research, grant RFBR-10-02-01443-a.

A The masses in the Higgs sector

The tree-level CP-even Higgs mass matrix in the basis (H_d^0, H_u^0, S) reads [53]

$$
\begin{aligned}
\left(\mathcal{M}_+^0\right)_{11} &= \left[\frac{({g_Y}^2+g_2^2)^2}{4} + Q_1^2 {g_1'}^2\right](vc_\beta)^2 + \frac{\lambda A_\lambda t_\beta v_s}{\sqrt{2}} \\
\left(\mathcal{M}_+^0\right)_{12} &= -\left[\frac{({g_Y}^2+g_2^2)^2}{4} - \lambda^2 - Q_1 Q_2 {g_1'}^2\right] v^2 s_\beta c_\beta - \frac{\lambda A_\lambda v_s}{\sqrt{2}} \\
\left(\mathcal{M}_+^0\right)_{13} &= \left[\lambda^2 + Q_1 Q'_S {g_{1'}}^2\right] v c_\beta v_s - \frac{\lambda A_\lambda v s_\beta}{\sqrt{2}} \\
\left(\mathcal{M}_+^0\right)_{22} &= \left[\frac{({g_Y}^2+g_2^2)^2}{4} + Q_2^2 {g_1'}^2\right](vs_\beta)^2 + \frac{\lambda A_\lambda v_s}{t_\beta \sqrt{2}} \\
\left(\mathcal{M}_+^0\right)_{23} &= \left[\lambda^2 + Q_2 Q'_S g_1^2\right] v s_\beta v_s - \frac{\lambda A_\lambda v c_\beta}{\sqrt{2}} \\
\left(\mathcal{M}_+^0\right)_{33} &= Q_S'^2 g_1'^2 v_s^2 + \frac{\lambda A_\lambda v^2 s_\beta c_\beta}{v_s \sqrt{2}},
\end{aligned}
\tag{28}
$$

The dominant radiative corrections due to top and stop are

$$
\begin{aligned}
(\mathcal{M}_+^1)_{11} &= k\left[\left(\frac{(\widetilde{m}_1^2)^2}{(m_{\tilde{t}_1}^2-m_{\tilde{t}_2}^2)^2}\mathcal{G}\right)(vc_\beta)^2+\left(\frac{\lambda h_t^2 A_t}{2\sqrt{2}}\mathcal{F}\right)t_\beta v_s\right]\\
(\mathcal{M}_+^1)_{12} &= k\left[\left(\frac{\widetilde{m}_1^2\widetilde{m}_2^2}{(m_{\tilde{t}_1}^2-m_{\tilde{t}_2}^2)^2}\mathcal{G}+\frac{h_t^2\widetilde{m}_1^2}{m_{\tilde{t}_1}^2+m_{\tilde{t}_2}^2}(2-\mathcal{G})\right)v^2 s_\beta c_\beta-\left(\frac{\lambda h_t^2 A_t}{2\sqrt{2}}\mathcal{F}\right)s\right]\\
(\mathcal{M}_+^1)_{13} &= k\left[\left(\frac{\widetilde{m}_1^2\widetilde{m}_s^2}{(m_{\tilde{t}_1}^2-m_{\tilde{t}_2}^2)^2}\mathcal{G}+\frac{\lambda^2 h_t^2}{2}\mathcal{F}\right)vc_\beta v_s-\left(\frac{\lambda h_t^2 A_t}{2\sqrt{2}}\mathcal{F}\right)vs_\beta\right]\\
(\mathcal{M}_+^1)_{22} &= k\left(\frac{(\widetilde{m}_2^2)^2}{(m_{\tilde{t}_1}^2-m_{\tilde{t}_2}^2)^2}\mathcal{G}+\frac{2h_t^2\widetilde{m}_2^2}{m_{\tilde{t}_1}^2+m_{\tilde{t}_2}^2}(2-\mathcal{G})+h_t^4\ln\frac{m_{\tilde{t}_1}^2 m_{\tilde{t}_2}^2}{m_t^4}\right)(vs_\beta)^2\\
&\quad+k\left(\frac{\lambda h_t^2 A_t}{2\sqrt{2}}\mathcal{F}\right)\frac{v_s}{t_\beta}\\
(\mathcal{M}_+^1)_{23} &= k\left[\left(\frac{\widetilde{m}_2^2\widetilde{m}_s^2}{(m_{\tilde{t}_1}^2-m_{\tilde{t}_2}^2)^2}\mathcal{G}+\frac{h_t^2\widetilde{m}_s^2}{m_{\tilde{t}_1}^2+m_{\tilde{t}_2}^2}(2-\mathcal{G})\right)vs_\beta v_s-\left(\frac{\lambda h_t^2 A_t}{2\sqrt{2}}\mathcal{F}\right)vc_\beta\right]
\end{aligned}
$$

$$
(\mathcal{M}_+^1)_{33} = k\left[\left(\frac{(\widetilde{m}_s^2)^2}{(m_{\tilde{t}_1}^2-m_{\tilde{t}_2}^2)^2}\mathcal{G}\right)v_s^2+\left(\frac{\lambda h_t^2 A_t}{2\sqrt{2}}\mathcal{F}\right)\frac{v^2 s_\beta c_\beta}{v_s}\right], \tag{29}
$$

where $k = 3/(4\pi)^2$, h_t is the top Yukawa coupling and

$$
\begin{aligned}
\mathcal{G} &= 2\left[1-\frac{m_{\tilde{t}_1}^2+m_{\tilde{t}_2}^2}{m_{\tilde{t}_1}^2-m_{\tilde{t}_2}^2}\log\left(\frac{m_{\tilde{t}_1}}{m_{\tilde{t}_2}}\right)\right]\\
\mathcal{F} &= \log\left(\frac{m_{\tilde{t}_1}^2 m_{\tilde{t}_2}^2}{\Lambda^4}\right)-\mathcal{G}(m_{\tilde{t}_1}^2, m_{\tilde{t}_2}^2)
\end{aligned} \tag{30}
$$

and

$$
\begin{aligned}
\widetilde{m}_1^2 &= h_t^2\mu\left(\mu - A_t t_\beta\right)\\
\widetilde{m}_2^2 &= h_t^2 A_t\left(A_t-\frac{\mu}{t_\beta}\right)\\
\widetilde{m}_s^2 &= \left(\frac{vc_\beta h_t}{v_s}\right)^2\mu(\mu - A_t t_\beta)
\end{aligned} \tag{31}
$$

The $\overline{\text{DR}}$ renormalization scale, Λ is fixed to 1 TeV. The CP-odd mass tree-level matrix reads

$$
\left(\mathcal{M}_-^0\right) = \frac{\lambda A_\lambda}{\sqrt{2}}\begin{pmatrix} t_\beta v_s & v_s & vs_\beta\\ v_s & \frac{v_s}{t_\beta} & vc_\beta\\ vs_\beta & vc_\beta & \frac{v^2 s_\beta c_\beta}{v_s}\end{pmatrix} \tag{32}
$$

(33)

and the one-loop corrections due to top and stop

$$(\mathcal{M}^1_-)_{ij} = \frac{\lambda v^2 s_\beta c_\beta v_s}{\sqrt{2} v_i v_j} \frac{k h_t^2 A_t}{2} \mathcal{F}, \quad i,j \in \{1,2,3\}, \tag{34}$$

where $v_1 = v_d, v_2 = v_u, v_3 = v_s$.

The charged Higgs mass including radiative corrections from the top and stop sector,

$$\begin{aligned} m^2_{H^\pm} &= \frac{\lambda A_\lambda \sqrt{2}}{\sin 2\beta} v_s - \frac{\lambda^2}{2} v^2 + M_W^2 + \Delta^2_{H+} \\ \Delta^2_{H+} &= \frac{\lambda A_t v_s k h_t^2 \mathcal{F}}{\sqrt{2} \sin 2\beta} + \frac{3 {g_2}^2}{32\pi^2 M_W^2} \left(\frac{2 m_t^2 m_b^2}{s_\beta^2 c_\beta^2} - M_W^2 \left(\frac{m_t^2}{s_\beta^2} + \frac{m_b^2}{c_\beta^2} \right) + \frac{2}{3} M_W^4 \right) \log \frac{\Lambda^2}{m_t^2} \end{aligned} \tag{35}$$

where the SUSY scale Λ is taken to be 1 TeV.

References

[1] H. Goldberg, *Constraint on the Photino Mass from Cosmology*, *Phys.Rev.Lett.* **50** (1983) 1419.

[2] J. R. Ellis, J. Hagelin, D. V. Nanopoulos, K. A. Olive, and M. Srednicki, *Supersymmetric Relics from the Big Bang*, *Nucl.Phys.* **B238** (1984) 453–476.

[3] L. Roszkowski, *Particle dark matter: A Theorist's perspective*, *Pramana* **62** (2004) 389–401, [hep-ph/0404052].

[4] H. Baer, E.-K. Park, and X. Tata, *Collider, direct and indirect detection of supersymmetric dark matter*, *New J.Phys.* **11** (2009) 105024, [arXiv:0903.0555].

[5] J. Ellis and K. A. Olive, *Supersymmetric Dark Matter Candidates*, arXiv:1001.3651.

[6] T. Falk, K. A. Olive, and M. Srednicki, *Heavy sneutrinos as dark matter*, *Phys.Lett.* **B339** (1994) 248–251, [hep-ph/9409270].

[7] **XENON100 Collaboration** Collaboration, E. Aprile *et al.*, *First Dark Matter Results from the XENON100 Experiment*, *Phys.Rev.Lett.* **105** (2010) 131302, [arXiv:1005.0380].

[8] **The CDMS-II Collaboration** Collaboration, Z. Ahmed *et al.*, *Dark Matter Search Results from the CDMS II Experiment*, *Science* **327** (2010) 1619–1621, [arXiv:0912.3592].

[9] R. Mohapatra, *Mechanism for understanding small neutrino mass in superstring theories* , *Phys.Rev.Lett.* **56** (1986) 561–563.

[10] R. Mohapatra and J. Valle, *Neutrino Mass and Baryon Number Nonconservation in Superstring Models*, *Phys.Rev.* **D34** (1986) 1642.

[11] T. Asaka, K. Ishiwata, and T. Moroi, *Right-handed sneutrino as cold dark matter*, *Phys. Rev.* **D73** (2006) 051301, [hep-ph/0512118].

[12] T. Asaka, K. Ishiwata, and T. Moroi, *Right-handed sneutrino as cold dark matter of the universe*, *Phys. Rev.* **D75** (2007) 065001, [hep-ph/0612211].

[13] S. Gopalakrishna, A. de Gouvea, and W. Porod, *Right-handed sneutrinos as nonthermal dark matter*, *JCAP* **0605** (2006) 005, [hep-ph/0602027].

[14] C. E. Yaguna, *Inverse decays and the relic density of the sterile sneutrino*, *Phys.Lett.* **B669** (2008) 139–144, [arXiv:0811.0485].

[15] N. Arkani-Hamed, L. J. Hall, H. Murayama, D. Tucker-Smith, and N. Weiner, *Small neutrino masses from supersymmetry breaking*, *Phys. Rev.* **D64** (2001) 115011, [hep-ph/0006312].

[16] F. Borzumati and Y. Nomura, *Low scale seesaw mechanisms for light neutrinos*, *Phys.Rev.* **D64** (2001) 053005, [hep-ph/0007018].

[17] J. March-Russell, C. McCabe, and M. McCullough, *Neutrino-Flavoured Sneutrino Dark Matter*, *JHEP* **03** (2010) 108, [arXiv:0911.4489].

[18] A. Kumar, D. Tucker-Smith, and N. Weiner, *Neutrino Mass, Sneutrino Dark Matter and Signals of Lepton Flavor Violation in the MRSSM*, *JHEP* **1009** (2010) 111, [arXiv:0910.2475].

[19] G. Belanger, M. Kakizaki, E. Park, S. Kraml, and A. Pukhov, *Light mixed sneutrinos as thermal dark matter*, *JCAP* **1011** (2010) 017, [arXiv:1008.0580].

[20] J. McDonald, *RH sneutrino condensate CDM and the baryon-to-dark matter ratio*, arXiv:0710.2360.

[21] L. J. Hall, T. Moroi, and H. Murayama, *Sneutrino cold dark matter with lepton-number violation*, *Phys. Lett.* **B424** (1998) 305–312, [hep-ph/9712515].

[22] C. Arina, F. Bazzocchi, N. Fornengo, J. Romao, and J. Valle, *Minimal supergravity sneutrino dark matter and inverse seesaw neutrino masses*, *Phys.Rev.Lett.* **101** (2008) 161802, [arXiv:0806.3225].

[23] H. An, P. Dev, Y. Cai, and R. Mohapatra, *Sneutrino Dark Matter in Gauged Inverse Seesaw Models for Neutrinos*, arXiv:1110.1366.

[24] P. Bandyopadhyay, E. J. Chun, and J.-C. Park, *Right-handed sneutrino dark matter in* $\mathbf{U(1)'}$ *seesaw models and its signatures at the LHC*, *JHEP* **1106** (2011) 129, [arXiv:1105.1652].

[25] H. N. Long, *Right-handed sneutrinos as self-interacting dark matter in supersymmetric economical 3-3-1 model*, *Adv.Stud.Theor.Phys.* **4** (2010) 173–196, [arXiv:0710.5833].

[26] C. Arina, *Sneutrino cold dark matter in extended MSSM models*, arXiv:0805.1991.

[27] D. G. Cerdeno and O. Seto, *Right-handed sneutrino dark matter in the NMSSM*, *JCAP* **0908** (2009) 032, [arXiv:0903.4677].

[28] D. A. Demir, L. L. Everett, M. Frank, L. Selbuz, and I. Turan, *Sneutrino Dark Matter: Symmetry Protection and Cosmic Ray Anomalies*, *Phys.Rev.* **D81** (2010) 035019, [arXiv:0906.3540].

[29] D. G. Cerdeno, J.-H. Huh, M. Peiro, and O. Seto, *Very light right-handed sneutrino dark matter in the NMSSM*, arXiv:1108.0978.

[30] Z. Kang, J. Li, T. Li, T. Liu, and J. Yang, *Asymmetric Sneutrino Dark Matter in the NMSSM with Minimal Inverse Seesaw*, arXiv:1102.5644.

[31] H.-S. Lee, K. T. Matchev, and S. Nasri, *Revival of the thermal sneutrino dark matter*, *Phys.Rev.* **D76** (2007) 041302, [hep-ph/0702223].

[32] P. Langacker, *The Physics of Heavy Z' Gauge Bosons*, *Rev.Mod.Phys.* **81** (2009) 1199–1228, [arXiv:0801.1345].

[33] M. Cvetic and P. Langacker, *Implications of Abelian extended gauge structures from string models*, *Phys.Rev.* **D54** (1996) 3570–3579, [hep-ph/9511378].

[34] P. Langacker, *Grand Unified Theories and Proton Decay*, *Phys.Rept.* **72** (1981) 185.

[35] J. L. Hewett and T. G. Rizzo, *Low-Energy Phenomenology of Superstring Inspired E(6) Models*, *Phys.Rept.* **183** (1989) 193.

[36] N. Arkani-Hamed, A. Cohen, E. Katz, and A. Nelson, *The Littlest Higgs*, *JHEP* **0207** (2002) 034, [hep-ph/0206021].

[37] T. Han, H. E. Logan, B. McElrath, and L.-T. Wang, *Phenomenology of the little Higgs model*, *Phys.Rev.* **D67** (2003) 095004, [hep-ph/0301040].

[38] U. Ellwanger, C. Hugonie, and A. M. Teixeira, *The Next-to-Minimal Supersymmetric Standard Model*, *Phys.Rept.* **496** (2010) 1–77, [arXiv:0910.1785].

[39] M. Cvetic, D. A. Demir, J. Espinosa, L. Everett, and P. Langacker, *Electroweak breaking and the mu problem in supergravity models with an additional U(1)*, *Phys.Rev.* **D56** (1997) 2861, [hep-ph/9703317].

[40] P. Langacker and J. Wang, *U(1)-prime symmetry breaking in supersymmetric E(6) models*, *Phys.Rev.* **D58** (1998) 115010, [hep-ph/9804428].

[41] A. Ahriche and S. Nasri, *Electroweak Phase Transition in the U(1)'-MSSM*, arXiv:1008.3106.

[42] V. Barger, P. Langacker, M. McCaskey, M. J. Ramsey-Musolf, and G. Shaughnessy, *LHC Phenomenology of an Extended Standard Model with a Real Scalar Singlet*, *Phys.Rev.* **D77** (2008) 035005, [arXiv:0706.4311].

[43] M. Bastero-Gil, C. Hugonie, S. King, D. Roy, and S. Vempati, *Does LEP prefer the NMSSM?*, *Phys.Lett.* **B489** (2000) 359–366, [hep-ph/0006198].

[44] J. Kalinowski, S. F. King, and J. P. Roberts, *Neutralino Dark Matter in the USSM*, *JHEP* **01** (2009) 066, [arXiv:0811.2204].

[45] B. de Carlos and J. Espinosa, *Cold dark matter candidate in a class of supersymmetric models with an extra U(1)*, *Phys.Lett.* **B407** (1997) 12–21, [hep-ph/9705315].

[46] V. Barger, P. Langacker, I. Lewis, M. McCaskey, G. Shaughnessy, *et al.*, *Recoil Detection of the Lightest Neutralino in MSSM Singlet Extensions*, *Phys.Rev.* **D75** (2007) 115002, [hep-ph/0702036].

[47] D. G. Cerdeno, C. Munoz, and O. Seto, *Right-handed sneutrino as thermal dark matter*, *Phys.Rev.* **D79** (2009) 023510, [arXiv:0807.3029].

[48] F. Deppisch and A. Pilaftsis, *Thermal Right-Handed Sneutrino Dark Matter in the F(D)-Term Model of Hybrid Inflation*, *JHEP* **0810** (2008) 080, [arXiv:0808.0490].

[49] C. Arina and N. Fornengo, *Sneutrino cold dark matter, a new analysis: Relic abundance and detection rates*, *JHEP* **0711** (2007) 029, [arXiv:0709.4477].

[50] R. Allahverdi, B. Dutta, K. Richardson-McDaniel, and Y. Santoso, *Sneutrino Dark Matter and the Observed Anomalies in Cosmic Rays*, *Phys. Lett.* **B677** (2009) 172–178, [arXiv:0902.3463].

[51] R. Allahverdi, S. Bornhauser, B. Dutta, and K. Richardson-McDaniel, *Prospects for Indirect Detection of Sneutrino Dark Matter with IceCube*, *Phys. Rev.* **D80** (2009) 055026, [arXiv:0907.1486].

[52] J. Erler, P. Langacker, S. Munir, and E. R. Pena, *Improved Constraints on Z' Bosons from Electroweak Precision Data*, *JHEP* **08** (2009) 017, [arXiv:0906.2435].

[53] V. Barger, P. Langacker, H.-S. Lee, and G. Shaughnessy, *Higgs Sector in Extensions of the MSSM*, *Phys.Rev.* **D73** (2006) 115010, [hep-ph/0603247].

[54] U. Ellwanger and C. Hugonie, *Masses and couplings of the lightest Higgs bosons in the (M+1) SSM*, *Eur.Phys.J.* **C25** (2002) 297–305, [hep-ph/9909260].

[55] U. Ellwanger, M. Rausch de Traubenberg, and C. A. Savoy, *Higgs phenomenology of the supersymmetric model with a gauge singlet*, *Z.Phys.* **C67** (1995) 665–670, [hep-ph/9502206].

[56] F. Franke and H. Fraas, *Mass bounds for the neutral Higgs bosons in the next-to-minimal supersymmetric standard model*, *Phys.Lett.* **B353** (1995) 234–242, [hep-ph/9504279].

[57] **CMS Collaboration** Collaboration, S. Chatrchyan *et al.*, *Search for standard model Higgs boson in pp collisions at 7TeV and integrated luminosity up to 1.7 fb^{-1}*, . CMS PAS HIG-11-022.

[58] G. Bélanger and J. Da Silva. in preparation.

[59] C. Collaboration, *Search for Supersymmetry at the LHC in Events with Jets and Missing Transverse Energy*, arXiv:1109.2352.

[60] **ATLAS Collaboration** Collaboration, G. Aad *et al.*, *Search for squarks and gluinos using final states with jets and missing transverse momentum with the ATLAS detector in sqrt(s) = 7 TeV proton-proton collisions*, arXiv:1109.6572.

[61] G. Aad, B. Abbott, J. Abdallah, A. A. Abdelalim, A. Abdesselam, *et al.*, *Search for dilepton resonances in pp collisions at sqrt(s) = 7 TeV with the ATLAS detector*, arXiv:1108.1582.

[62] **Particle Data Group** Collaboration, K. Nakamura *et al.*, *Review of particle physics*, *J.Phys.G* **G37** (2010) 075021.

[63] S. Bertolini, F. Borzumati, A. Masiero, and G. Ridolfi, *Effects of supergravity induced electroweak breaking on rare B decays and mixings*, *Nucl.Phys.* **B353** (1991) 591–649.

[64] F. Domingo and U. Ellwanger, *Updated Constraints from B Physics on the MSSM and the NMSSM*, *JHEP* **0712** (2007) 090, [arXiv:0710.3714].

[65] G. Belanger, F. Boudjema, P. Brun, A. Pukhov, S. Rosier-Lees, *et al.*, *Indirect search for dark matter with micrOMEGAs2.4*, *Comput.Phys.Commun.* **182** (2011) 842–856, [arXiv:1004.1092].

[66] A. Semenov, *LanHEP - a package for automatic generation of Feynman rules from the Lagrangian. Updated version 3.1*, arXiv:1005.1909.

[67] A. Pukhov, *Calchep 2.3: MSSM, structure functions, event generation, 1, and generation of matrix elements for other packages*, hep-ph/0412191.

[68] G. Belanger, F. Boudjema, A. Pukhov, and A. Semenov, *micrOMEGAs2.0: A program to calculate the relic density of dark matter in a generic model*, *Comput. Phys. Commun.* **176** (2007) 367–382, [hep-ph/0607059].

[69] G. Belanger, F. Boudjema, A. Pukhov, and A. Semenov, *Dark matter direct detection rate in a generic model with micrOMEGAs2.1*, *Comput. Phys. Commun.* **180** (2009) 747–767, [arXiv:0803.2360].

[70] J. Giedt, A. W. Thomas, and R. D. Young, *Dark matter, the CMSSM and lattice QCD*, *Phys. Rev. Lett.* **103** (2009) 201802, [arXiv:0907.4177].

[71] **WMAP Collaboration** Collaboration, E. Komatsu *et al.*, *Seven-Year Wilkinson Microwave Anisotropy Probe (WMAP) Observations: Cosmological Interpretation*, *Astrophys.J.Suppl.* **192** (2011) 18, [arXiv:1001.4538].

[72] V. Barger, P. Langacker, and H.-S. Lee, *Primordial nucleosynthesis constraints on Z' properties*, *Phys.Rev.* **D67** (2003) 075009, [hep-ph/0302066].

[73] **WMAP Collaboration** Collaboration, E. Komatsu *et al.*, *Five-Year Wilkinson Microwave Anisotropy Probe (WMAP) Observations: Cosmological Interpretation*, *Astrophys.J.Suppl.* **180** (2009) 330–376, [arXiv:0803.0547].

[74] L. M. Krauss, C. Lunardini, and C. Smith, *Neutrinos, WMAP, and BBN*, *Phys.Rev.D* (2010) [arXiv:1009.4666].